RADIO CORPORATION OF AMERICA
RCA LABORATORIES

FIRST SEMIANNUAL REPORT

RADIATION DAMAGE TO SILICON

CONTRACT NO. NAS5-457

NATIONAL AERONAUTICS AND SPACE ADMINISTRATION

GODDARD SPACE FLIGHT CENTER

REPORT DATE: JANUARY 1, 1962

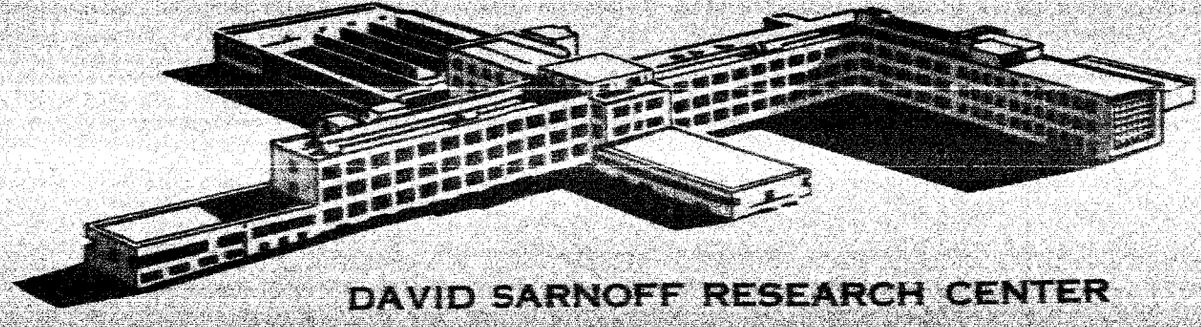

DAVID SARNOFF RESEARCH CENTER

PRINCETON, NEW JERSEY

Title Suppl. → FIRST SEMIANNUAL REPORT
2nd Copy.

~~Covering the Period:~~ July 1, 1961 to January 1, 1962

Report Date: January 1, 1962

Title **RADIATION DAMAGE TO SILICON**

(NASA CONTRACT ~~NO.~~ NAS 5-457)

~~NATIONAL AERONAUTICS AND SPACE ADMINISTRATION~~

~~GODDARD SPACE FLIGHT CENTER, Greenbelt, Md.~~

Rept. → (NASA CR-51044;

Report Prepared by: J. A. Baicker,
B. W. Faughnan,
R. L. Novak, and
J. J. Wysocki

Jan. 1, 1962 43 p 20 refs

Report Approved by: P. Rappaport, Project Supervisor

TABLE OF CONTENTS

ABSTRACT

21178

This report describes the first results of an investigation into the basic properties of the radiation-induced defects in silicon. The report is divided into four main sections dealing, respectively, with measurements of excess carrier lifetimes, majority-carrier concentrations and mobilities, electron spin resonance, and thermally stimulated conductivity. Lifetime measurements are described; the methods include pulse-injection, solar cell spectral response, and pulsed Van-de-Graaff injection. Lifetime vs temperature data indicate a defect level in n-type silicon located 0.18 ev below the conduction band. Evidences of trapping are described, and results using material from commercial solar cells are discussed. Resistivity-mobility measurements in n-type silicon confirm the location of a defect level at the same position in the band gap, but the indentity of the recombination and carrier-removal centers at this position is inconclusive. The last two parts of the program have been confined to development of techniques and equipment; both electron spin resonance and thermally stimulated conductivity require high instrumental resolution and sensitivity. Spin resonances associated with the previously known defects in n-type silicon have been seen and are described.

PURPOSE

The objective of this program is a better understanding of the basic properties of the defects that are produced in silicon and other semiconductors by nuclear radiation. The ultimate goal is a reduction of the radiation damage susceptibility of devices such as solar cells that are made from these materials.

I. INTRODUCTION

The discovery in 1958 of the Van-Allen radiation surrounding the earth has stimulated a great deal of research and engineering effort on the problems of radiation damage to semiconductor materials and devices. Among semiconductor devices the most damage susceptible are those which, like solar cells, depend on long minority carrier lifetimes or diffusion lengths. In earlier work under the present contract an extensive study was made of the deterioration which silicon solar cells experienced under monoenergetic electron, proton, alpha particle, and ultraviolet irradiation. The results of this investigation have been reported in detail in previous reports. Although ample statistics were obtained on the damage rate as a function of all measurable cell parameters, no conclusive criteria could be found by means of which damage resistant cells could be selected from an average group of cells. The current effort reflects a change in emphasis from the original device-property study to an investigation of the basic characteristics of radiation defects in silicon. Several phases of the study, including electron-spin resonance, resistivity-mobility, and minority carrier lifetime, will be described in the following sections of this report. In addition to these phases preparatory work has been done on studies of surface metallography, thermally stimulated low temperature conductivity and mass spectrographic analysis.

II. LIFETIME

THEORETICAL DISCUSSION

A straightforward formulation of the generation-recombination process in semiconductors when the recombination occurs through energy levels in the forbidden gap leads to a set of coupled differential equations which describe the rate at which recombination occurs in terms of the excess carrier concentrations, recombination center concentration, capture cross section, etc. Although early treatments of the problem date back at least to 1939, the first studies which resulted in solutions to the equations under certain restricted conditions did not appear until the well-known results of Hall[1] and Shockley and Read[2] were published in 1952. Shockley-Read treated the case of equilibrium generation-recombination via a single recombination level, for the special case of small injection and low concentration of recombination centers. These early theoretical studies provided the stimulus for a great deal of subsequent experimental and theoretical work. Exact solutions to the transient recombination problem have been found under small injection conditions, and approximate solutions for moderately high injection levels. The case of two independent types of center existing simultaneously has been studied, and a single center having several ionization states both within the forbidden gap has been considered with the help of electronic computers.

In the notation of Shockley and Read,* which is now uniformly adopted, the capture rates for electrons and holes are given by

$$U_n = N_t \langle \sigma_n v_e \rangle [(1 - f_t) n_o - f_t n_1]$$
$$U_p = N_t \langle \sigma_p v_h \rangle [f_t p_o - (1 - f_t) p_1] \qquad (1)$$

On the assumption that the injection level is low and the trap concentration is small compared with the majority carrier concentration they obtained an expression for the lifetime under equilibrium excitation-recombination conditions.

$$\tau_p = \frac{\tau_o + (\tau_{no} + \tau_{po}) \frac{\Delta p}{n_o}}{1 + \frac{\Delta p}{n_o}} \qquad (2)$$

* See page 19 for a list of definitions of the symbols used.

where τ_o, the lifetime under vanishingly small injection is given by

$$\tau_o = \tau_{po}\left(\frac{n_o + n_1}{n_o + p_o}\right) + \tau_{no}\left(\frac{p_o + p_1}{n_o + p_o}\right) \tag{3}$$

These expressions and what follows are specifically for n-type material; the equivalent expressions for p-type are obtained by interchange of n and p subscripts.

Under similarly restrictive assumptions regarding the signal level and trap concentration Sandiford[3] has obtained an expression for the transient lifetime,

$$\tau_p = \frac{\tau_{no}[p_o + p_1 + N_t^-] + \tau_{po}[n_o + n_1 + N_t^o]}{n_o + p_o + \dfrac{N_t^- N_t^o}{N_t}} \tag{4}$$

and under moderately high injection conditions the expression obtained by Wertheim[4] is

$$\tau_p = \frac{\tau_{po} + \tau_{no}\dfrac{(p_1 + N_t)}{n_o} + (\tau_{po}\,\Delta n + \tau_{no}\,\Delta p)\left(n_o + p_o + \dfrac{N_t^- N_t^o}{N_t}\right)^{-1}}{\left[1 + \dfrac{n_o\,\Delta n}{n_o + n_1} + \dfrac{p_o\,\Delta p}{p_o + p_1}\right] \Big/ (n_o + p_o + N_t^- N_t^o / N_t)} \tag{5}$$

If more than one type of independent center is present, then one would expect the resulting lifetime to be

$$\frac{1}{\tau} = \sum_i \frac{1}{\tau_i} \tag{6}$$

where

$$\frac{1}{\tau_i} = \frac{1 + \dfrac{\Delta p}{n_o}}{\tau_{o_i} + (\tau_{no_i} + \tau_{po_i})\dfrac{\Delta p}{n_o}} \tag{7}$$

Blakemore[5] has been able to obtain good experimental fits between lifetime measurements made in boron-doped p-type silicon and equations (6) and (7).

For ordinary silicon in the extrinsic region the factors n_o and p_o are practically temperature independent. The lifetime terms τ_{po} and τ_{no} have a slow temperature dependence (varying approximately as $T^{1/2}$) but the chief temperature variations occur in n_1 and p_1

$$n_1 = \tfrac{1}{2} N_c e^{-(E_c - E_t)/kT}$$

$$p_1 = \tfrac{1}{2} N_v e^{-(E_t - E_v)/kT} \qquad (8)$$

N_c and N_v also have a slow ($T^{3/2}$) temperature variation, but the resulting lifetimes in (2), (3), (4) or (6) are dominated by the exponential terms in (8).

In previous reports a series of lifetime measurements which were made by observing the reverse transient behavior of p-n junctions was described. In this method the junction is given a large current pulse in the forward direction, and the decay of the open circuit voltage immediately following the current pulse obeys the relation $V = V_o - \frac{kT}{e} \frac{t}{\tau}$.[6] This method provides a quick and convenient measurement of the minority carrier lifetime in the lighter-doped side of the junction, but unfortunately requires a high injection level in the region immediately next to the junction. A second method of determining the minority carrier lifetime by measuring the diffusion length was also described; this consisted of fitting the spectral response curves of shallow-junction solar cells to the theory of Loferski and Wysocki,[7] from which the diffusion length in the base region of the cell could be calculated. The fact that the minority carrier lifetimes determined by these two methods did not always agree was possibly due to the low injection level under which the spectral response was measured, and possibly due to the fact that one measurement yields the transient lifetime, and the other gives the lifetime under equilibrium excitation-recombination conditions.

Since there has been considerable theoretical treatment of the excess-carrier lifetime, both for the simple case of low injection, and a single recombination level, and for more general situations, a considerable portion of the effort in the present contract has been directed to a study of the behavior of the lifetime as a function of irradiation flux, sample temperature, and injection level in samples of silicon of various resistivities and impurity constituents.

As a part of this program the RCA 1 Mev electron Van-de-Graaff has been converted pulsed-beam operation by the addition of a post-acceleration electrostatic deflection system. Using a mercury switch pulser to provide the deflection pulses the system is capable of complete beam switching in times of the order of 10^{-9} second, limited only by the transit time of the electron beam through the deflection plates. In its present form the system provides two additional methods for lifetime measurement: observing the decay of the bombardment-induced conductivity and the decay of the open-circuit junction electro-voltage. Both methods have been examined, and a number of both n-type and p-type silicon specimens have been studied in detail using the bombardment-conductivity decay method. Most of the samples were in the 1-3 ohm-cm resistivity range, which was chosen to allow a comparison with pervious published results.

The pulsed-beam system is shown schematically in Fig. 1 and some representative conductivity-decay curves are shown in Fig. 2.

The results of lifetime vs temperature measurements on a number of samples are shown in Figs. 3 through 9. Several interesting features are immediately apparent. Figures 3 and 4, for example, show two specimens that were cut from the same original crystal but in different thicknesses. The initial lifetimes are different in the two cases (in the .018" specimen τ was in excess of one microsecond; in the .005" sample it was about 0.4 microsecond). This difference is taken to be an indication of the importance of surface recombination in the unirradiated thin specimens, and probably also in the thick specimens. The behavior after irradiation is relatively similar in the two cases, provided there are sufficient defects introduced for bulk recombination to dominate surface recombination. The sample shown in Fig. 3 was measured before irradiation and after two successive exposures each amounting to 1.0×10^{15} electrons per cm^2. The sample shown in Fig. 4 was exposed first to 2.5×10^{14} and then to 5×10^{14} electrons/cm^2. The activation energies appear to be slightly different in the two samples (0.15 and 0.17-0.18 ev) but there was no apparent change in ΔE in either sample on the two successive irradiations.

Figure 5 shows the results that were obtained with two specimens of arsenic-doped material. The preirradiation curves for the two are practically coincident, the post-irradiation activation energies are the same, and the magnitudes of the post-irradiation lifetime are consistent with the measured fluxes in the two cases.

Figure 6 shows two different pieces that were cut from the base of a commercial p/n solar cell, one of which was proton-irradiated and one of which was electron-irradiated. Two points should be noted with regard to these samples: the defect level appears to be the same in the two cases, and is lower in energy (0.10 to 0.11 ev) than in other n-type samples that were studied. This particular cell was found to be unusually damage-susceptible during the proton irradiation ($\phi_c = 9 \times 10^9$ protons/cm^2). The combination of low lifetime activation energy and high solar cell damage susceptibility may be significant, and will be the subject of additional measurements as the work progresses.

Figure 7 shows the results in phosphorus-doped material, and Fig. 8 shows pulse-injection results in another proton-irradiated cell.

A sample of high resistivity n-type material was studied for comparison with the 1-3 ohm-cm material. This sample showed strong evidence of single-level trapping (see Fig. 9) which masked the recombination center behavior.

A complete analysis of the lifetime measurements will require data on the manner in which the injection level influences the results, but a rough picture of the final result may be obtained from an examination of the relatively low-level injection shown in the previous figures. From equations (2) and (3), in n-type silicon the lifetime vs temperature should obey either

$$\tau = \tau_{po}\left(1 + \frac{n_1}{n_o}\right) \tag{9}$$

if the defect level lies in the upper half of the band gap or

$$\tau = \tau_{po}\left(1 + \frac{\tau_{no}}{\tau_{po}} \frac{p_1}{n_o}\right) \tag{10}$$

if the defect level lies in the lower half of the band gap.

In the case of Fig. 4, for example, the results can best be accounted for in terms of equation (9), which suggests that the defect lies in the vicinity of 0.17 ev below the bottom of the conduction band. This result is in agreement with the results of Galkin et al[8] and in disagreement with Wertheim.[9]

In addition to a more conclusive identification of the position of the major defect level, the lifetime vs injection level measurement are important to verify the nature of the recombination process (single level vs multiple level, for example).

III. RESISTIVITY-MOBILITY

APPARATUS

The equipment designed for low temperature irradiations of samples is described below. The apparatus permits the viewing of the beam distribution over the area occupied by the sample, measurement of the electron beam current in a Faraday cup, rapid insertion and extraction of the sample from the beam and interruption of the beam during measurements of the Hall constant in situ. A cross-section diagram of the apparatus is shown in Fig. 10. The principal parts of the apparatus are identified by letters.

Section A is a auxilliary cooling jacket which surrounds the main dewar resevoir B. The sample is surrounded by copper radiation shields; one extending downward from A and the other at D. These radiation shields are slotted so that they also act as a beam collimator. A resistance heater E permits the copper sample mounting strip F to be heated above the temperature of the bath.

The sample mounting strip contains two holes across one of which the sample is mounted and the other is lifted back to permit observation of the beam profile. Either one of these holes can be positioned in the electron beam by means of the double bellows G and spring P. The spring is able to support the structure in its upper position when the space between the bellows is filled with air at atmospheric pressure. When this space is evacuated during bombardment, the bellows contract, and the dewar A is lowered, and therefore the sample holder moves to a position where the first hole is exposed to the electron beam. When the upper bellows M is evacuated by a forepump, the pressure is equalized between M and G causing the springs P to raise the dewar and position the sample holder so that the first hole is exposed to the electron beam. The system can be cycled rapidly between these two positions by means of an electrically operated valve which alternately exposes the space between the bellows M to the atmosphere and to the forepump vacuum.

A electromagnet O whose axis is concentric with the beam permits measurements of Hall coefficient. At suitable intervals of flux the beam is interupted by means of the shutter L and measurements of the Hall coefficient and electrical resistivity are made.

ELECTRON RESULTS

The silicon crystals used in these experiments were grown from quartz crucibles by the usual Czochralski method. Experiments are also being done on floating zone 'n' and 'p' silicon which have a much lower oxygen content for comparison with these results.

The specimens were ultrasonically cut into standard Hall bridges such that the (111) face was normal to the axis of the bombarding particle. The specimens were polished to the final sizes since measurements were less erratic than with etched surfaces. Ohmic contact to the specimen was accomplished by alloying dots onto the arms of the specimen and then soldering the measuring wires directly to these arms. Temperature of the specimen was determined by soldering a thermocouple to one arm of the specimen. Using Freon 22 for cooling the electrical resistivity and Hall coefficient were measured at 240°K before bombardment. Bombardment with electron fluxes of $\sim 2 \times 10^{14}$ electrons/cm^2/sec, heated the specimens very rapidly so that the bombarding temperature was 300°K. After the electron beam was interrupted the measurements were repeated when the temperature had dropped to the reference point.

For detecting small changes in carrier concentration the electrical resistivity is more sensitive than the Hall coefficient. If we assume the mobility is not changed by small bombardments the change in carrier concentration $\Delta n = \Delta\sigma/e\mu$. The number of carriers removed is $n_o(\rho_1 - \rho_o)/\rho_1$ where n_o is the initial carrier concentration and ρ_o and ρ_1 are the respective resistivities before and after bombardment. The assumption of bombardment independent mobility seems to be justified for the temperatures and carrier concentrations employed here. Changes of 30% in the carrier concentration determined in the above manner produced no detectable change in the Hall mobility. However, at lower temperatures where charged impurity scattering becomes more important than lattice scattering the Hall mobility and hence the conductivity mobility drops markedly with bombardment. At liquid nitrogen temperature the carrier removal rate must be calculated from changes in the Hall coefficient.

Prior to bombardment at the higher energies the specimens were subjected to a 'conditioning' bombardment at energies below the threshold for bulk damage. Changes in the electrical conductivity occur here and are thought to be due to changes in the surface states.

Figure 11 shows the carrier removal in n-type silicon bombarded with 300 KEV electrons. Figure 12 is the same plot for p-type silicon, but it should be noted that the abscissa is compressed by a factor of ten. However, the carrier removal rate is not necessarily the same as the defect introduction rate. The position of the Fermi level determines the number

of removal centers that are occupied, the determination of which requires carrier concentration measurements as a function of temperature. Also, even though the removal sites may all be occuppied, the total number of carriers removed is less at temperatures below the saturation range. When this condition prevails the ratio of the carrier concentration before and after bombardment is more important than the number of carriers removed.

The temperature dependence of carrier concentration for n-type silicon before and after irradiation is shown in Fig. 13. In the unirradiated sample the impurity donors remain ionized down to ~ 150°K which produces an essentially constant carrier concentration. After irradiation a "step," which is a measure of the acceptors introduced, appears in the curve. As the temperature decreases, the Fermi level moves toward the conduction band and in doing so it "sweeps" through the defect level responsible for carrier removal. The defect level fills up and in doing so removes electrons from the conduction band. In non-degenerate material

$$n = N_c \exp[(\epsilon_f - \epsilon_d)/kT] \tag{11}$$

Then the number of defect sites occupied by electrons is

$$N_t^- = \frac{N_t}{1 + \exp[(\epsilon_t - \epsilon_f)/kT]} \tag{12}$$

where ϵ_t is the energy of the defect level. In the saturation region the number of carriers measured by the Hall constant

$$R_H = r/nec \tag{13}$$

is $n = N_D - N_t \sim N_D$ if material is not heavily compensated. When defects are introduced the measured carrier concentration is $n = N_D - N_t^-$. By combining these three equations we get a quadratic in n: $n^2 + (N_t - N_D + N_c\, e^x)\, n - N_c\, N_D\, e^x = 0$ where $x = (\epsilon_t - \epsilon_c)/kT$. The expression may be used to solve for $\epsilon_t - \epsilon_c$. For simplicity we can calculate this ΔE in the following manner. When $\epsilon_f = \epsilon_t$

$$n = N_c \exp[(\epsilon_t - \epsilon_c)/kT] \text{ and } n = N_D - \frac{N_t}{2}$$

so that

$$ln\left[\frac{N_c}{N_D - N_t/2}\right] = \frac{\epsilon_c - \epsilon_t}{kT} \tag{14}$$

and by determining the temperature at which half filling of the traps occurs the energy level is obtained directly. The value obtained for the removal level is $E_c - 0.19$ ev at 240°K. At this temperature only 38% of the removal sites are effective in removing carriers. For p-type material the level lies deeper in the gap, $\sim (E_v + .30)$ ev, and the removal sites are always filled at this temperature. Figure 14 shows the rate at which carrier removal centers are introduced in n and p-type silicon assuming each center captures one carrier. For the 300 KEV electrons the damage rate as measured by the introduction of carrier removal centers is about an order of magnitude greater in n-type than in p-type. The respective introduction rates for n and p type silicon being 8.7×10^{-3} cm^{-1} and 7.45×10^{-4} cm^{-1}.

PROTON RESULTS

Specimens of n and p-type silicon were irradiated with 1.7 Mev protons to a total flux of 5×10^{14} protons/cm^2. Figures 15 and 16 show the reciprocal of the Hall constant plotted against temperature. As a result of bombardment the curves are displaced downward due to the introduction of carrier removal centers. The removal sites are filled completely even at room temperature, and the ratio of carrier concentrations before and after bombardment remains very nearly constant with temperature. Therefore, this suggests that the carrier removal sites must lie further than 0.20 from either band edge in both n and p-type material. Although the fraction of carriers removed, 40% of the original carrier concentration, is about the same for both the n and p samples, the p-type had a larger number of carriers removed than the n-type. The introduction rate for p and n-type being 5.3 cm^{-1} and 1.7 cm^{-1}. This is in contrast with electron damage where the n-type rate is an order of magnitude higher than the p-type rate. Proton damage measurements are being repeated and extended to determine where the removal levels are positioned and to check the introduction rates.

Figure 17 shows the ratio of the Hall constant before bombardment to that after bombardment (or alternatively the ratio of carrier concentration after bombardment to that before) for proton and electron bombarded n-type silicon. Both had about the same carrier concentration before bombardment $\sim 1.5 \times 10^{15}$ elec./cm^3. The difference between the two as described above is well illustrated.

IV. ELECTRON SPIN RESONANCE OF IRRADIATION DEFECT CENTERS IN SEMICONDUCTORS

INTRODUCTION

The electron spin resonance spectra of irradiation defect centers in semiconductors have many properties in common with ESR (electron spin resonance) spectra observed in unirradiated material. Therefore, a brief survey of ESR in unirradiated semiconductors will be given.

The first resonance observed in silicon was that of free electrons[10] and electrons bound to shallow donor impurities.[11] The latter resonance arises from the extra donor electron which does not take part in the covalent bonding of the crystal and it is only observed at low temperatures when the donor atoms are deionized. The observed resonance corresponds to an electron spin $S = 1/2$ and has a g value close to the free electron value.

In addition the single line corresponding to $S = 1/2$ is split by the hyperfine interaction of the donor nucleus. For example, the resonance spectra of the phosphorus donor which has a nuclear spin $I = 1/2$ consists of two lines separated by 43 gauss. The As donor with $I = 3/2$ has a four line spectrum. There is a further hyperfine interaction between the donor electron and the surrounding Si^{29} nuclei. This interaction is responsible for the linewidth of the donor resonances. This is a characteristic of inhomogeneously broadened lines. The spin-lattice relaxation and dipole-dipole interaction limited line-width is very small. However, the randomly oriented nuclear spins of the Si^{29} nuclei produce a much larger linewidth for the overall system of spins.

The spin lattice relaxation times of the donor electrons is very long at low temperatures (seconds to hours in the liquid helium range). The saturation behavior of such systems has been studied by Portis.[12] The imaginary or absorption component of the r.f. susceptibility saturates very easily but the dispersion component does not saturate. Therefore, the dispersion signal is invariably measured in these studies. Portis also shows that if magnetic field modulation is used the recorder will trace out an absorption curve rather than the usual derivative of a dispersion curve, at least if the external experimental parameters are adjusted for adiabatic fast passage conditions.

The unresolved hyperfine structure of the Si^{29} nuclei has been resolved by Feher[13] using the electron nuclear double resonance technique (ENDOR).

Early attempts to observe hole resonance or resonance of acceptors in semiconductors were unsucessful. However, more recent attempts have succeeded.[14],[15] In order to observe acceptor resonances it is necessary to apply a uniaxial strain to the crystal to remove the degeneracy of valence band at $k = 0$. It has been shown that this degenercy will lead to a broadening of the acceptor resonance linewidth to the extent that observation of acceptor resonance is impossible unless this degeneracy is removed.

The first studies of irradiation damage centers were carried out by Bemski[16] and Watkins et al[17] in electron irradiated n-type silicon. The dominant center which appears in pulled n-type Si was thoroughly studied by Watkins and Corbett, who named it the SiA-center. They showed that the defect was connected with oxygen impurities present in the pulled crystal. According to their model an interstitial oxygen atom combines with a vacancy created by electron irradiation to produce a substitutional oxygen defect. Spin resonance of this defect is observable because the defect can accept on electron which gives rise to spin resonance. This corresponds to a net acceptor level .17 ev below the conduction band. In order for the resonance to be observable the temperature must be sufficiently low so that electrons from the donor atom drop down to the defect level.

The work of Watkins and Corbett demonstrated the importance of impurities in the formation of stable damage centers at room temperature. They found that for floating zone Si which contains less oxygen than pulled Si ($\sim 10^{16}$ per cm^3 compared to $\sim 10^{18}$ cm^3 for pulled Si) the A-center did not appear. A new center which they called the SiE-center is created and is identified as a defect arising from a donor atom-vacancy combination.[18] They identify a third type defect which does not depend on impurities present in the crystal. This is the divancy (Si C- and Si J-center), a stable combination of two vacancies. At room temperature the number of these defects is only 5% of the Si A-center defects in pulled n-type Silicon.

A limitation on the ESR technique for studying radiation damage is that the defect must be able to accept an unpaired electron for the observation of spin resonance. It should be possible to observe a defect with a hole (by analogy with the observation of spin resonance of holes bound to acceptors); no such defect resonance has been observed as yet, however.

Another technique for studying radiation damage is the observation of ESR due to transition metal impurities in semiconductors before and after irradiation. In this case the resonance arises from the paramagnetism of the *d* shell of the transition metal and does not necessarily depend on accepting an extra electron at low temperatures. The effect of radiation damage would be observable through the change in the ESR spectrum brought about by the change in crystal environment of the impurity, presumably through vacancy-impurity interaction.

EXPERIMENTAL

SENSITIVITY CONSIDERATIONS

The nature of ESR resonance of irradiation produced defects requires the use of a high sensitivity spectrometer. For example, to observe the Si A-center, electrons must be supplied by the donor atoms. Thus, the maximum observable number of A-centers is equal to the number of donor atoms. For 1 ohm-cm Si this is $N_D \approx 5 \times 10^{15}/cm^3$. The amount of Si material used is limited by reasonable irradiation times and the perturbation of the Si on the microwave cavity. A typical volume of Si used in this work is 0.1 cm^3. Therefore, the number of defect centers = 5×10^{14}.

The sensitivity of ESR spectrometers is usually specified as the minimum detectable number of spins observable at room temperature using the maximum or most favorable microwave power. Under these conditions our spectrometer using homodyne operation and a magnetic field modulation frequency of 400 cps has a sensitivity such that

$$N_{min} = 2 \times 10^{12} \Delta H$$

where N_{min} = minimum detectable number of spins for a signal to noise ratio $S/N = 1$, and a filter time constant of 3 seconds.

ΔH = linewidth in gauss

The above figure was determined by measuring the signal to noise ratio of the resonance from a small ruby crystal with a known Cr concentration.

When the spectrometer is used to study radiation damage defects the sensitivity is reduced in several ways. In general, lower power levels must be used because of saturation effects. Furthermore, the magnitude of the susceptibility signal depends on external experimental parameters, such as magnitude and frequency of magnetic field modulation and rate of magnetic field sweep and it is not always possible to operate under conditions where the susceptibility signal is maximum.

In order to increase the sensitivity a superheterodyne system was recently added to the spectrometer. This allows operation at low power levels while still maintaining good sensitivity. Also,it reduces the amount of crystal noise reaching the detection amplifier. As yet the sensitivity obtainable using the superheterodyne system has not been equal to its theoretical value. The problem seems to be noise introduced by vibrations in the system, particularly with liquid helium leaking into the microwave cavity. These problems will be

pursued further. However, the sensitivity of the instrument is now sufficient for the study of irradiation defects of comparable density to the A-center. For this center the signal to noise ratio now obtained is approximately 100.

EXPERIMENTAL RESULTS

Most of the experimental work to date has been on n-type pulled Si crystals. In this material the dominant defect is the Si A-center. The phosphorus donor resonance in n-type 1 ohm-cm silicon is shown in Fig. 18. The two phosphorus hyperfine lines are separated by 43 gauss and have a linewidth of approximately 3 gauss. The resonance line between the phosphorus lines is from a small sample of DPPH used to calibrate the spectrometer sensitivity. At room temperature this DPPH sample has a signal to noise ration of 300.

Figure 19 shows the same phosphorus samples after irradiation with 800 KEV electrons, $\phi = 5 \times 10^{16}$ electrons/cm^2. The samples were .010" thick and irradiated on both sides to insure uniform irradiation damage. It can be seen that the phosphorus hyperfine lines are reduced in magnitude and the Si A-center defect now appears between the two phosphorus lines. Further irradiation would increase the magnitude of the phosphorus resonance as electrons bound to phosphorus atoms drop down to the A-center. The sharp line in the middle of the A-center is from conduction electrons in a small (0.3 mg) sample of Si doped with 10^{18} phos/cm^3. It is used as a field marker and for spectrometer calibration.

Figure 20 shows the A-center for a sample of As-doped Si irradiated with 800 KEV electrons with $\phi = 10^{17}$ elec/cm^3. Here the A-center resonance is considerably larger than the four As hyperfine lines also present in the sample. In the figures shown the structure of the A-center due to non-equivalent sets of atom sites is not resolved. The reason for this is not yet known.

A sample of n-type Si was irradiated with 2 mev protons with a flux of 5×10^{13} proton/cm^2. No defect resonance was found. However, the donor resonance was also not observed and it is felt that the sample was too small and the sensitivity too low to observe spin resonance. Further proton irradiation on larger Si samples will be carried out.

A small sample of n-type GaAs was also irradiated with 800 KEV electrons, $\phi = 10^{17}$ elec/cm^2. GaAs is peculiar in that the donor electrons remain in the conduction band even at liquid helium temperatures. This means that if a sufficiently large sample is used to observe resonance the microwave losses of the conduction electrons decrease the cavity Q to the extent that observation of ESR is impossible. The GaAs was irradiated in the hope that a defect level created by the irradiation would trap all the conduction electrons thereby raising

the resistivity of the sample. It was found, however, that the GaAs sample still remained excessively lossy at liquid helium temperature. However, it is felt that for this irradiation a significant fraction of the sample area was not covered by the electron beam and hence would remain lossy. The experiment will be tried again making sure that the entire area of GaAs is exposed to the beam.

FUTURE WORK

So far the experimental work has mostly been concerned with the A-center with emphasis on improving the sensitivity of the spectrometer. In the future work. emphasis will be placed on the correlation of spin resonance data with other measurements on irradiated Si, particularly lifetime measurements at room temperature. For example, one can ask, is the A-center, which is the dominant defect observed by ESR in n-type pulled Si for electron fluxes $\sim 10^{17}$ cm^2, also responsible for recombination in Si at room temperature at low flux levels of say 10^{14} cm^2. It is possible that at these low flux levels other impurities present in the crystal may be more important in creating lifetime limiting defects. A way of studying this problem and at the same time studying new radiation defects is to dope Si with known impurities, for example the transition elements, and to observe changes in the ESR spectra of these impurities with irradiation. Such changes would occur if the impurity is involved with the formation of a radiation defect.

A search will also be made for ESR spectra from defects produced by proton irradiation, in order to see what differences there are with respect to electron produced defects. This is important to the comparisons made between the two types of irradiation.

V. THERMALLY STIMULATED CONDUCTIVITY

Thermally stimulated light emission was first used as an important tool in the study of trapping processes in photoconductors in the immediate post-war years.[19] In these studies the specimens were cooled and sufficient carriers were generated by light to fill the existing traps. As the temperature was raised (with the light removed) the Fermi level moved through a portion of the energy gap, and those levels which the Fermi level traversed, emitted their trapped carriers. Light was observed as the carriers subsequently recombined. From the struc- of the "glow curves" (light emission vs temperature during the heating cycle) the energy levels and concentrations of the traps may be calculated.

A variation of the "glow curve" method has been utilized in more recent studies of photoconductors, when the sample is heated the excess conductivity due to thermal stimulation of charge carriers from the traps is observed.[20] Although this method has not yet been applied to the study of radiation defects in semiconductors it is ideally suited for observing defects lying in the same half of the band gap as the Fermi level, and an effort is being made to utilize it in measurements of high-resistivity silicon. In addition, since gallium arsenide is of interest and available in much higher resistivities than silicon this material will also be studied.

Most of the equipment required for this study is standard laboratory apparatus, and is being assembled. A specially constructed dewar is available for the study, and is presently being tested for temperature range and heating rate.

VI. SUMMARY AND FUTURE PLANS

The lifetime investigation is now yielding information that is of fundamental importance both to the damage process is silicon and to the operation of solar cells. Tentative locations of defect energy levels have been determined from the present data. A rapid accumulation of additional data, both on more samples and on the injection level dependence in the present samples will help to clarify the results in three specific regards. There is still some uncertainty in the tentative finding that the dominant level in n-type silicon lies in the upper half of the band gap, and the use of the single-level theory requires additional confirmation. There is considerable interest also in the apparent difference between the behavior of laboratory-grade silicon and samples of similar resistivity and doping that were prepared from commercial solar cells.

The carrier-removal experiments indicate defect levels which correspond roughly to those seen in the lifetime work, but additional data will be necessary before a conclusive correspondance can be established.

The development of a system for the study of electron spin resonance in irradiated silicon has been a major task, and is now nearing completion. The ultimate capability of the apparatus, both in sensitivity and resolution, is required. Future work in this area will be concentrated on intensive study of the defects that can be isolated. The inherent resolution of the spectrometer will suffice to isolate several of the defects, but selective annealing and heavy doping of samples with known impurities will be utilized.

REFERENCES

1. R. N. Hall, Phys. Rev. **87**, 387 (1952).
2. W. Shockley and W. T. Read, Jr., Phys. Rev. **87**, 835 (1952).
3. D. J. Sandiford, Phys. Rev. **105**, 524 (1957).
4. G. K. Wertheim, Phys. Rev. **109**, 1086 (1958).
5. J. S. Blakemore, Phys. Rev. **110**, 1301 (1958).
6. S. R. Lederhandler and L. J. Giacoletto, Proc. IRE **43**, 477 (1955).
   B. Lax and S. F. Neustadter, J. Applied Phys. **25**, 1148 (1954).
   J. C. Henderson and J. R. Tillman, Proc. I.E.E. **104B**, 318 (1957).
   W. H. Ko, IRE Transactions P.G.E.D., **ED8**, 123 (1961).
7. J. J. Loferski and J. J. Wysocki, RCA Review **22**, 38 (1961).
8. G. N. Galkin, N. S. Rytova, and V. S. Vavilov, Fizika Tverdovo Tela, **Vol. 2**, 2025 (1960).
9. G. K. Wertheim, Phys. Rev. **105**, 1730 (1957), also J. Applied Phys. **30**, 1166 (1959).
10. A. M. Portis, A. F. Kip, C. Kittel and W. H. Brattain, Phys. Rev. **90**, 988 (1953).
11. R. C. Fletcher, W. Yager, G. L. Pearson and F. R. Merrit, Phys. Rev. **95**, 844 (1954).
12. A. M. Portis, Phys. Rev. **91**, 1071 (1953).
13. G. Feher, Phys. Rev. **114**, 1219 (1959).
14. G. Feher, Proc. Int'l. Conference on Semiconductors, Prague, (1960).
15. G. Feher, J. C. Hansel, and E. A. Gere, Phys. Rev. Letters **5**, 309 (1960).
16. G. Bemski, J. Applied Physics **30**, 1195 (1959).
17. G. D. Watkins, J. W. Corbett and R. M. Walker, J. Applied Phys. **30**, 1198 (1959).
18. G. D. Watkins and J. W. Corbett, to be published.
19. J. T. Randall and M. H. F. Wilkins, Proc. Royal Soc. (London) **A184**, 366 (1945), ibid., 390 (1945).
20. J. Blanc, R. H. Bube and H. MacDonald, J. Applied Phys. **32**, 1666 (1961).

LIST OF SYMBOLS

$n_o ; p_o$	Thermal equilibrium concentration of electrons and holes.
N_t	Concentration of recombination centers
$N_t^- ; N_t^o$	Concentration of centers occupied by electrons and holes, respectively. $N_t^- = f_t N_t ; N_t^o = (1 - f_t) N_t$
$n_1 ; p_1$	Concentration of electrons and holes when the Fermi Level lies at the recombination level.
$\Delta n ; \Delta p$	Excess concentrations of electrons and holes.
$\sigma_n ; \sigma_p$	Capture cross sections of centers for electrons and holes, respectively.
τ_{no}	Lifetime of excess electrons in strongly p-type material.
τ_{po}	Lifetime of excess holes in strongly p-type material.
$v_e ; v_h$	Thermal velocities of electrons and holes.

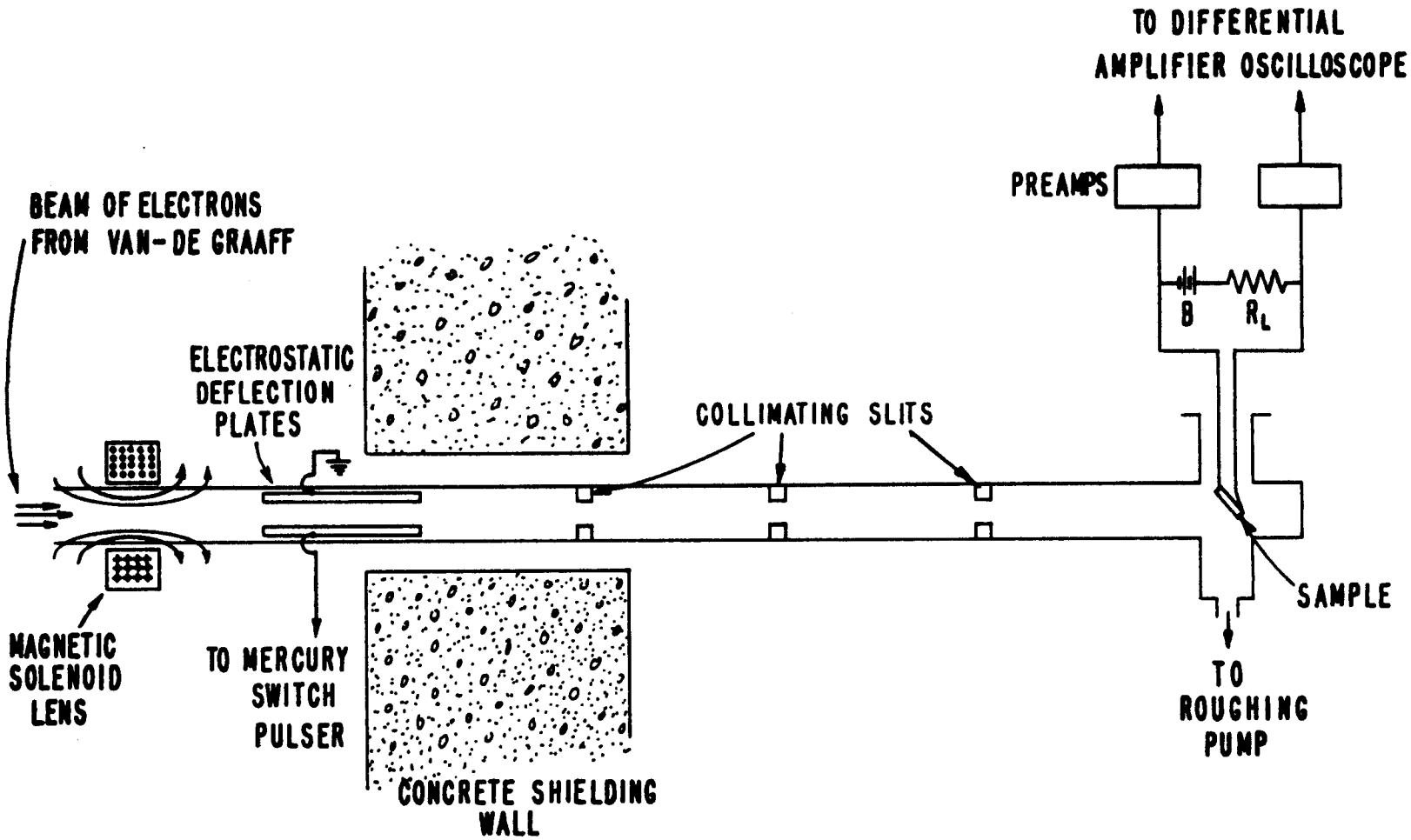

FIG. 1 SCHEMATIC DRAWING OF PULSED ELECTRON BEAM LIFETIME MEASURING APPARATUS.

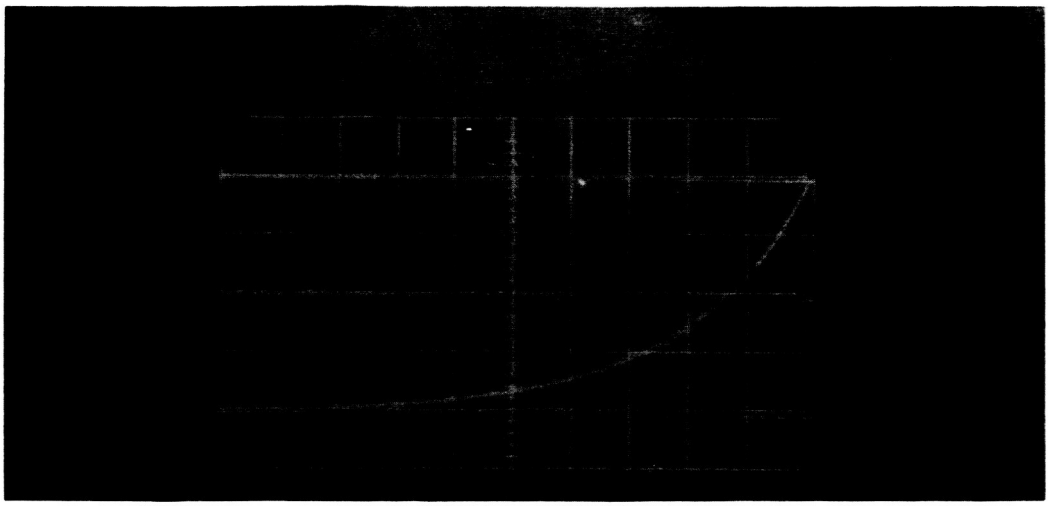

FIG. 2. TYPICAL OSCILLOSCOPE PHOTOGRAPH SHOWING CURRENT DECAY AND REFERENCE EXPONENTIAL CURVE.

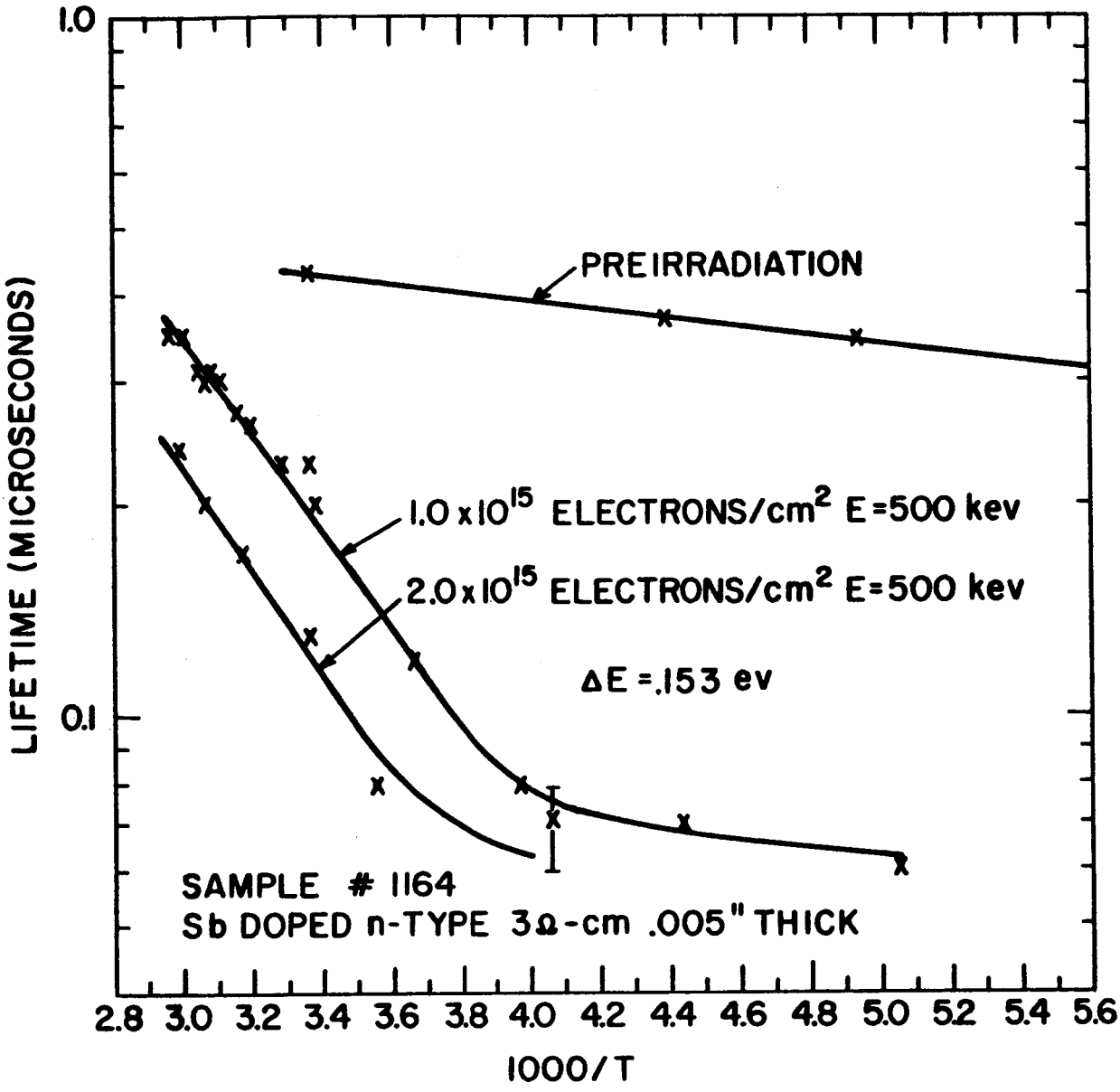
1.0
0.1
LIFETIME (MICROSECONDS)
PREIRRADIATION
1.0 x 10^15 ELECTRONS/cm^2 E=500 kev
2.0 x 10^15 ELECTRONS/cm^2 E=500 kev
ΔE = .153 ev
SAMPLE # 1164
Sb DOPED n-TYPE 3Ω-cm .005" THICK
2.8 3.0 3.2 3.4 3.6 3.8 4.0 4.2 4.4 4.6 4.8 5.0 5.2 5.4 5.6
1000/T

FIG. 3

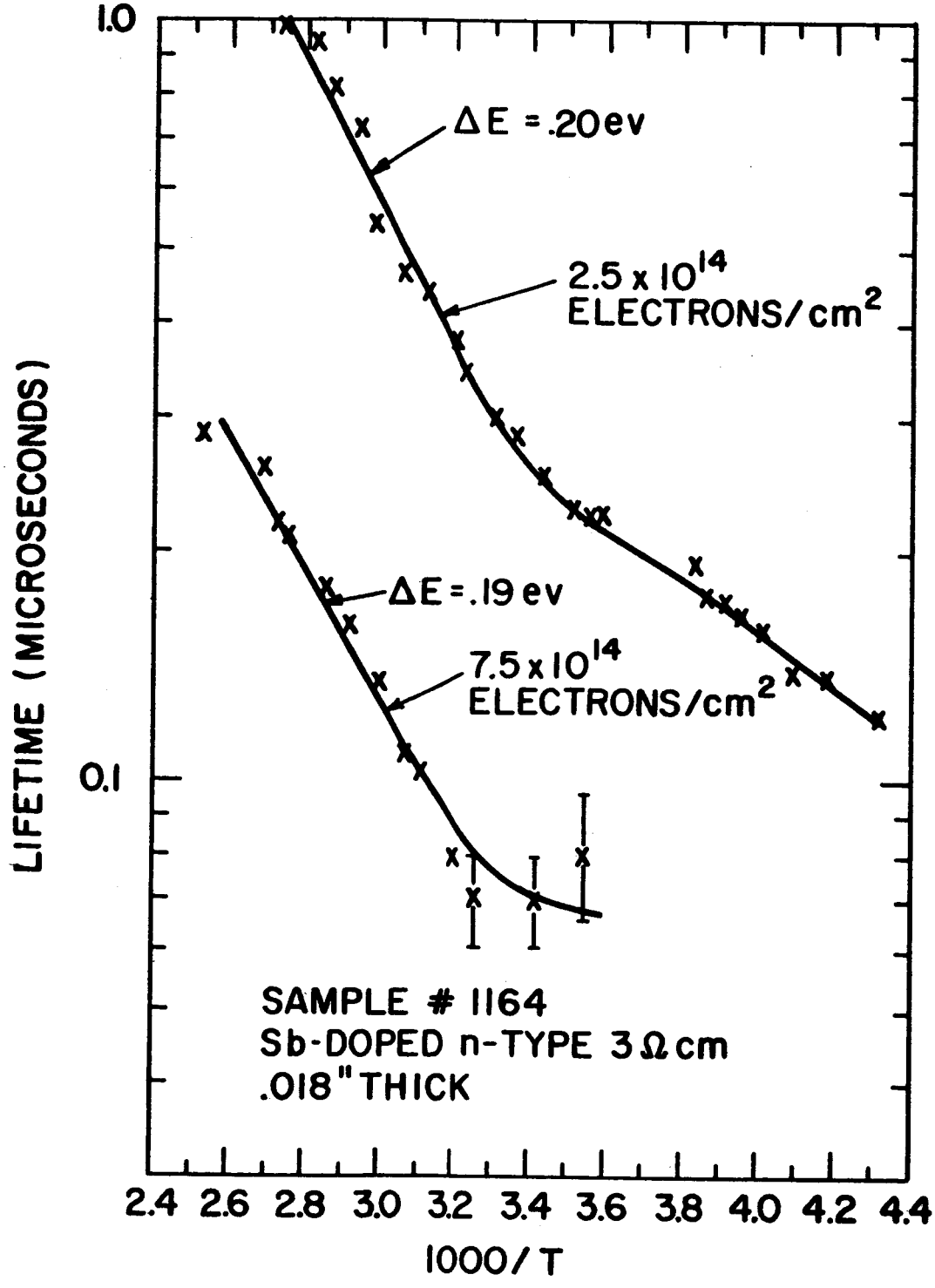
1.0
0.1
LIFETIME (MICROSECONDS)
ΔE = .20ev
2.5 x 10^14
ELECTRONS/cm^2
ΔE = .19 ev
7.5 x 10^14
ELECTRONS/cm^2
SAMPLE # 1164
Sb-DOPED n-TYPE 3 Ω cm
.018" THICK
2.4 2.6 2.8 3.0 3.2 3.4 3.6 3.8 4.0 4.2 4.4
1000/T

FIG. 4

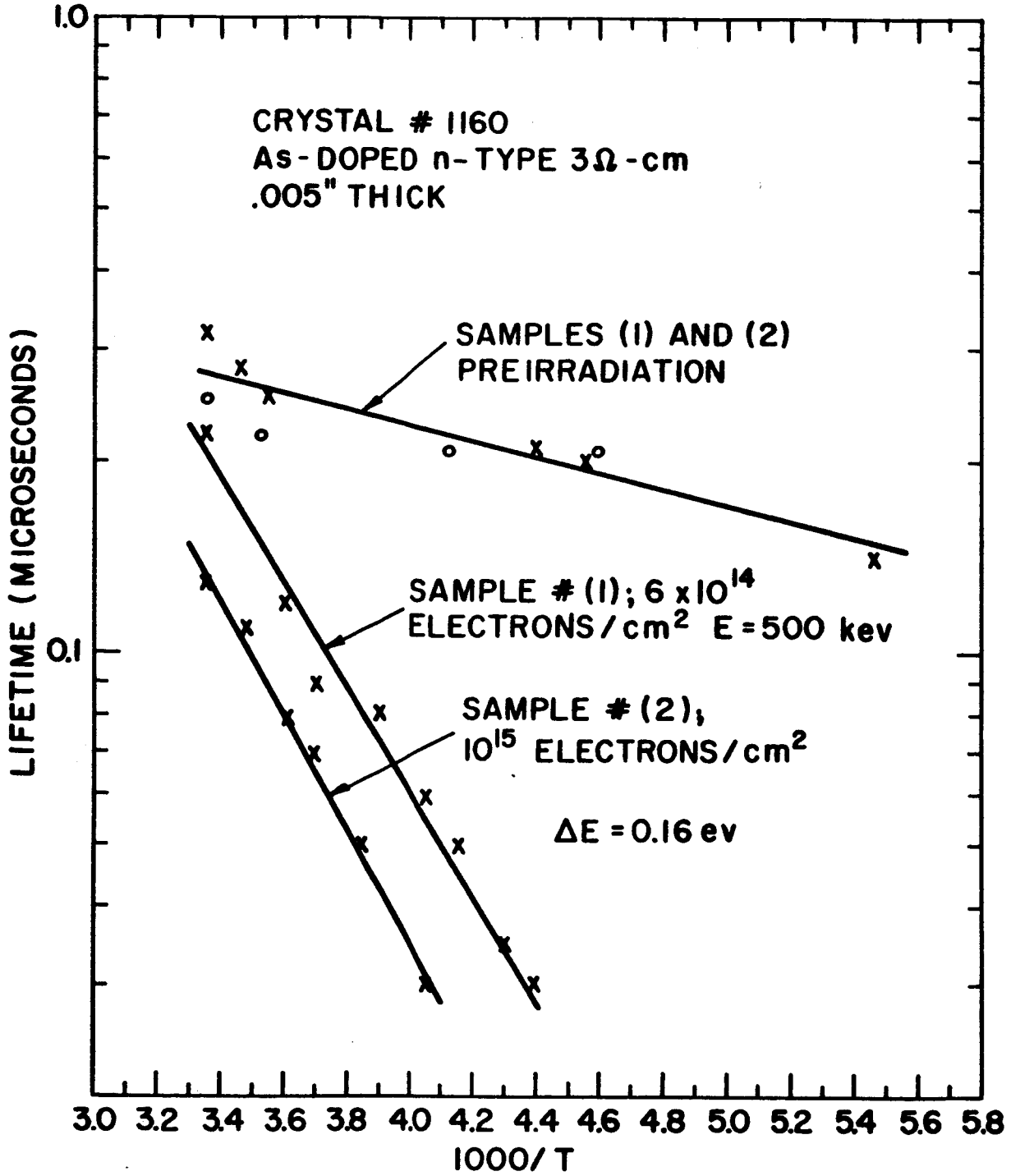
1.0
0.1
LIFETIME (MICROSECONDS)
CRYSTAL # 1160
As-DOPED n-TYPE 3Ω-cm
.005" THICK
SAMPLES (1) AND (2)
PREIRRADIATION
SAMPLE # (1); 6 x 10^14
ELECTRONS / cm^2 E = 500 kev
SAMPLE # (2);
10^15 ELECTRONS / cm^2
ΔE = 0.16 ev
3.0 3.2 3.4 3.6 3.8 4.0 4.2 4.4 4.6 4.8 5.0 5.2 5.4 5.6 5.8
1000/T

FIG.5

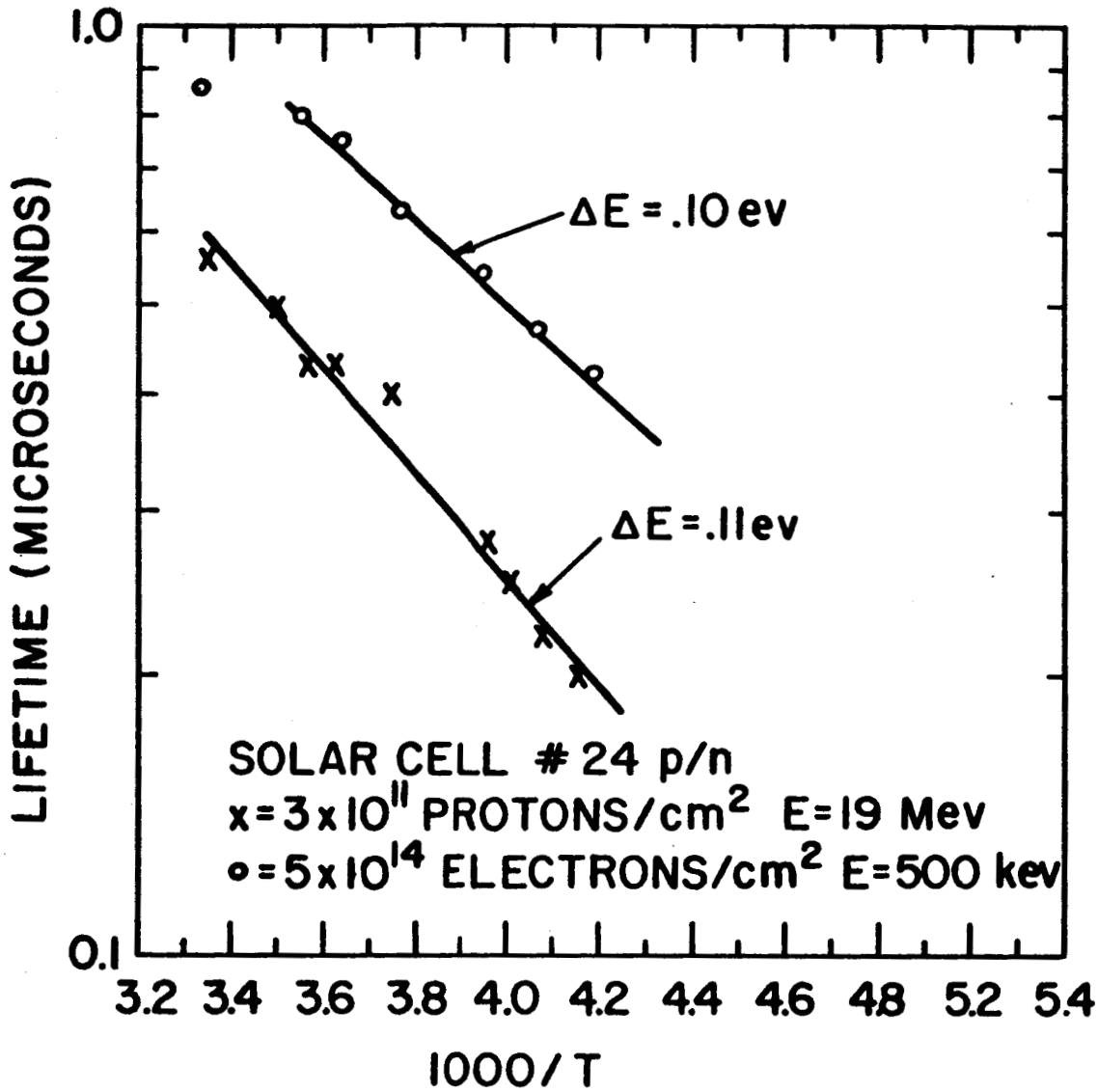
1.0
0.1
LIFETIME (MICROSECONDS)
ΔE = .10 ev
ΔE = .11 ev
SOLAR CELL # 24 p/n
x = 3 x 10^11 PROTONS/cm^2 E = 19 Mev
o = 5 x 10^14 ELECTRONS/cm^2 E = 500 kev
3.2 3.4 3.6 3.8 4.0 4.2 4.4 4.6 4.8 5.2 5.4
1000/T

FIG. 6

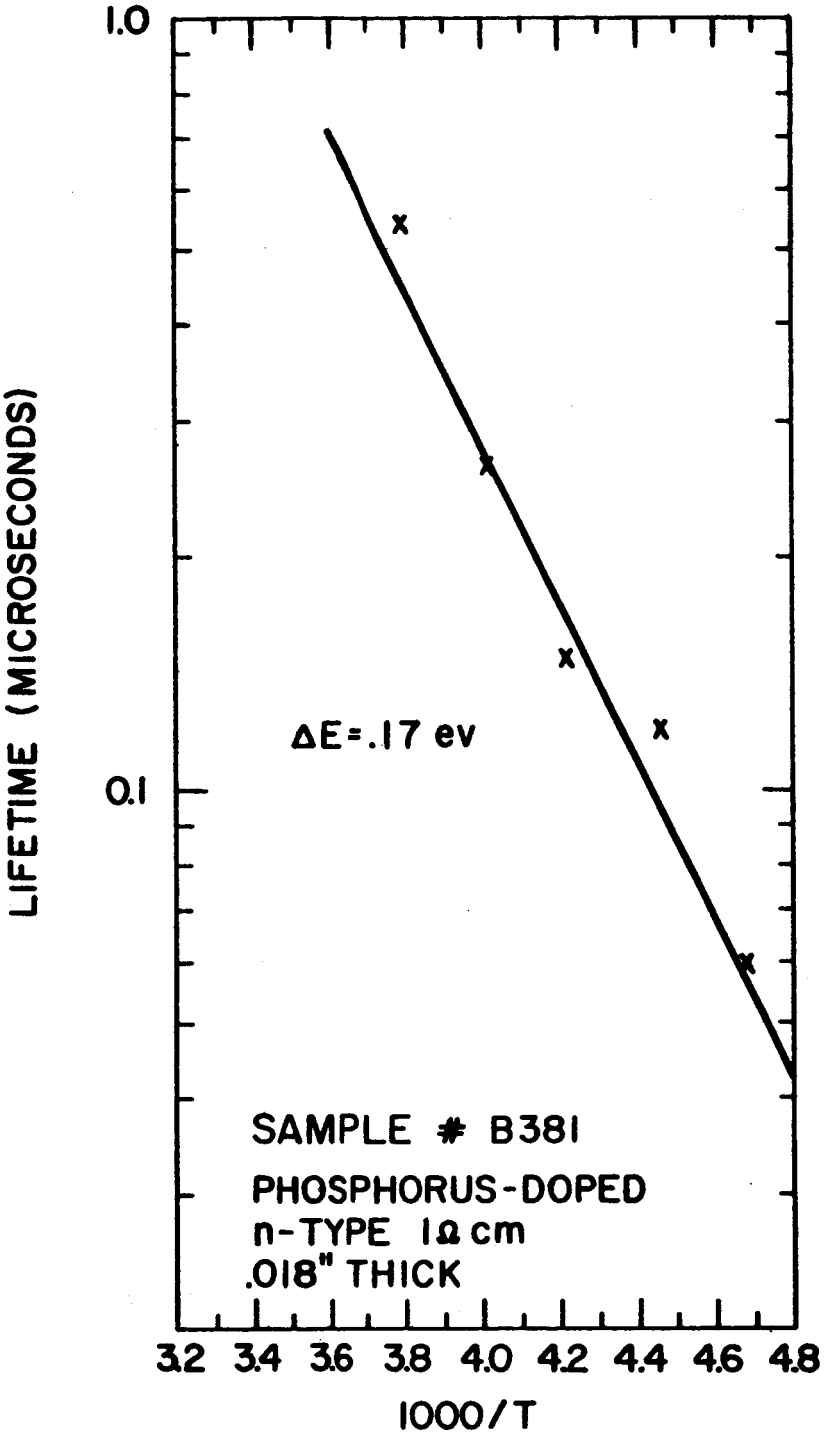
1.0
0.1
LIFETIME (MICROSECONDS)
ΔE=.17 ev
SAMPLE # B381
PHOSPHORUS-DOPED
n-TYPE 1Ω cm
.018" THICK
3.2 3.4 3.6 3.8 4.0 4.2 4.4 4.6 4.8
1000/T

FIG.7

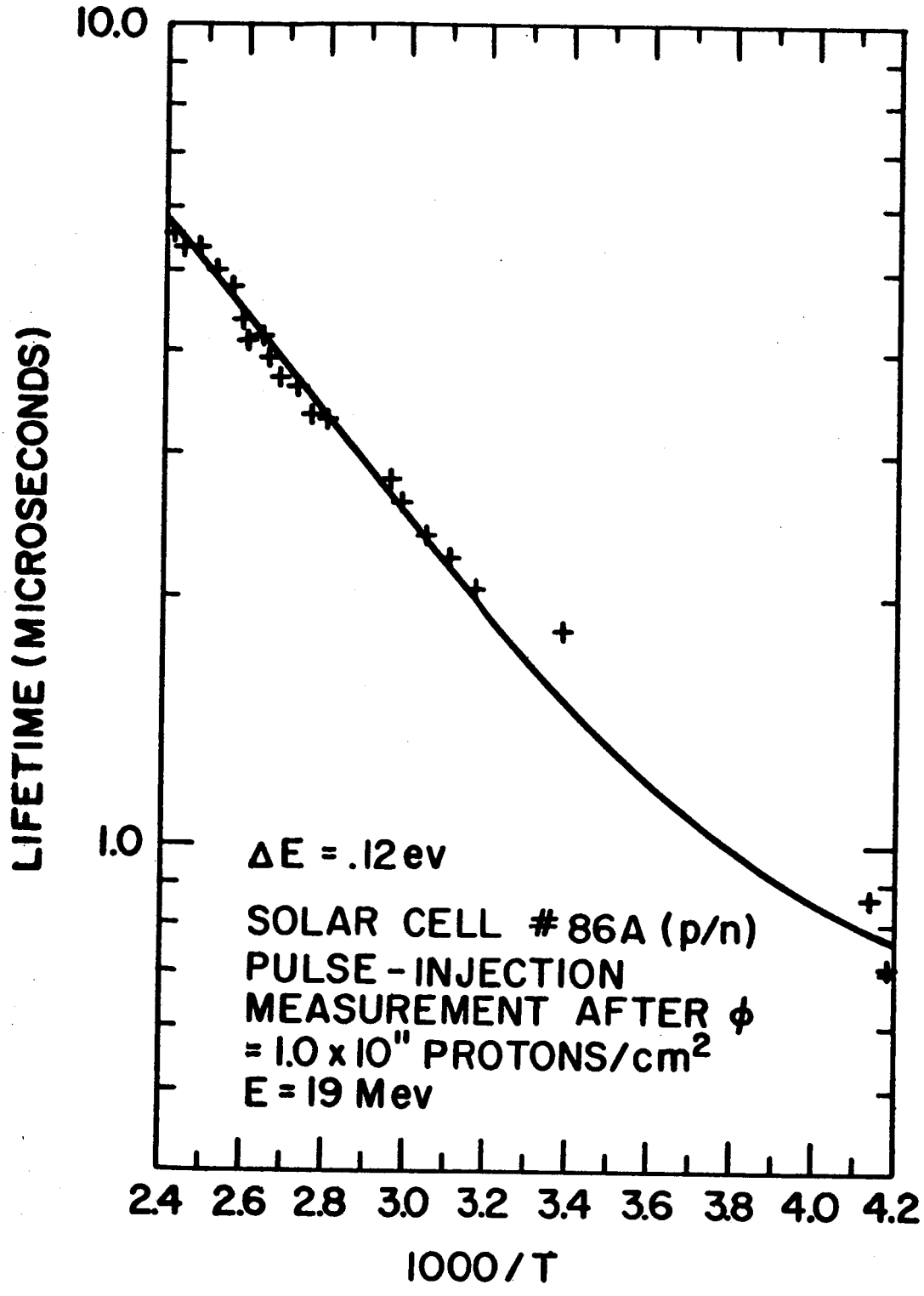
10.0
1.0
LIFETIME (MICROSECONDS)
ΔE = .12 ev
SOLAR CELL #86A (p/n)
PULSE-INJECTION
MEASUREMENT AFTER φ
= 1.0 x 10" PROTONS/cm²
E = 19 Mev
2.4 2.6 2.8 3.0 3.2 3.4 3.6 3.8 4.0 4.2
1000/T

FIG. 8

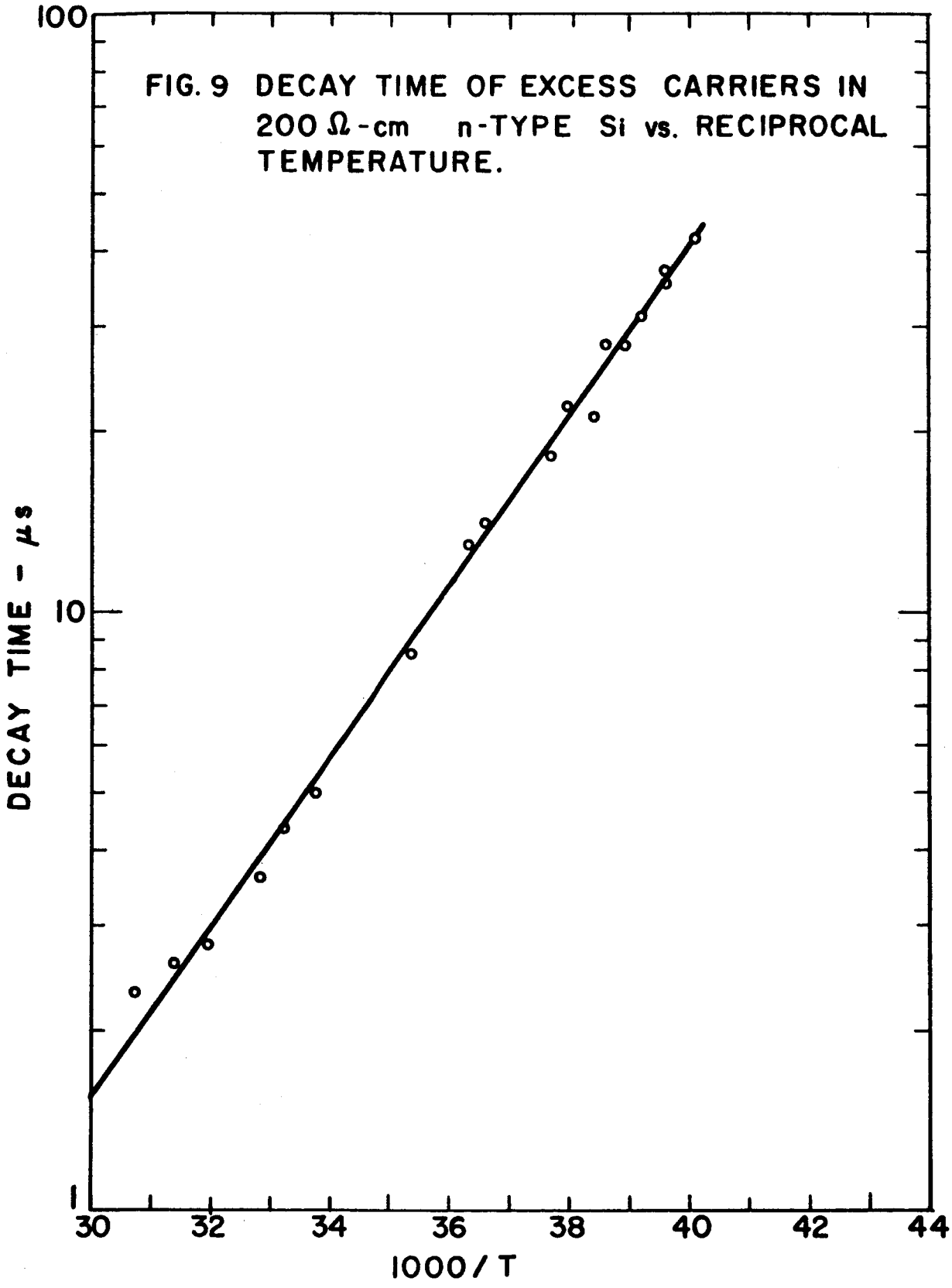

FIG. 9 DECAY TIME OF EXCESS CARRIERS IN 200 Ω-cm n-TYPE Si vs. RECIPROCAL TEMPERATURE.

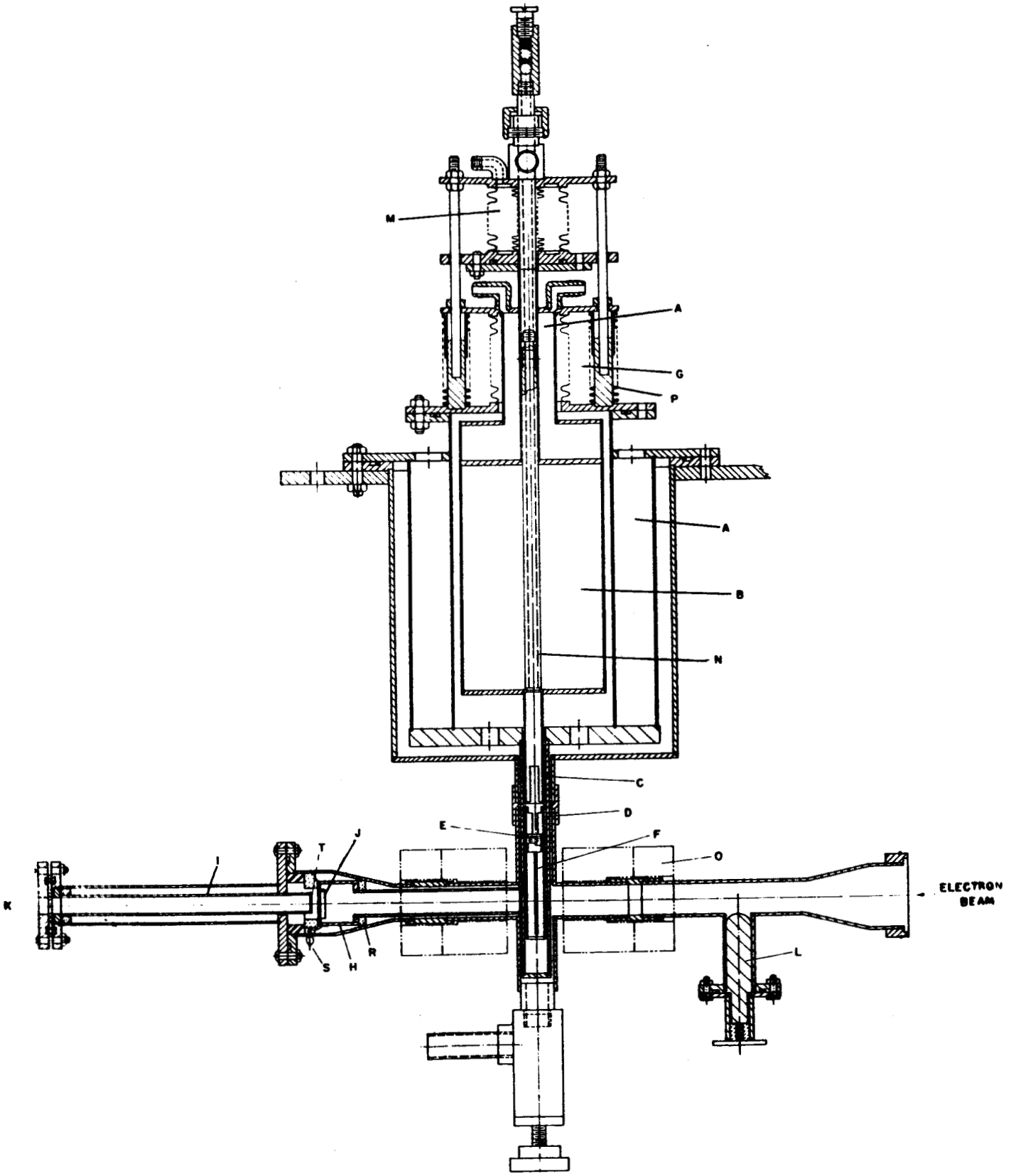

FIG. 10

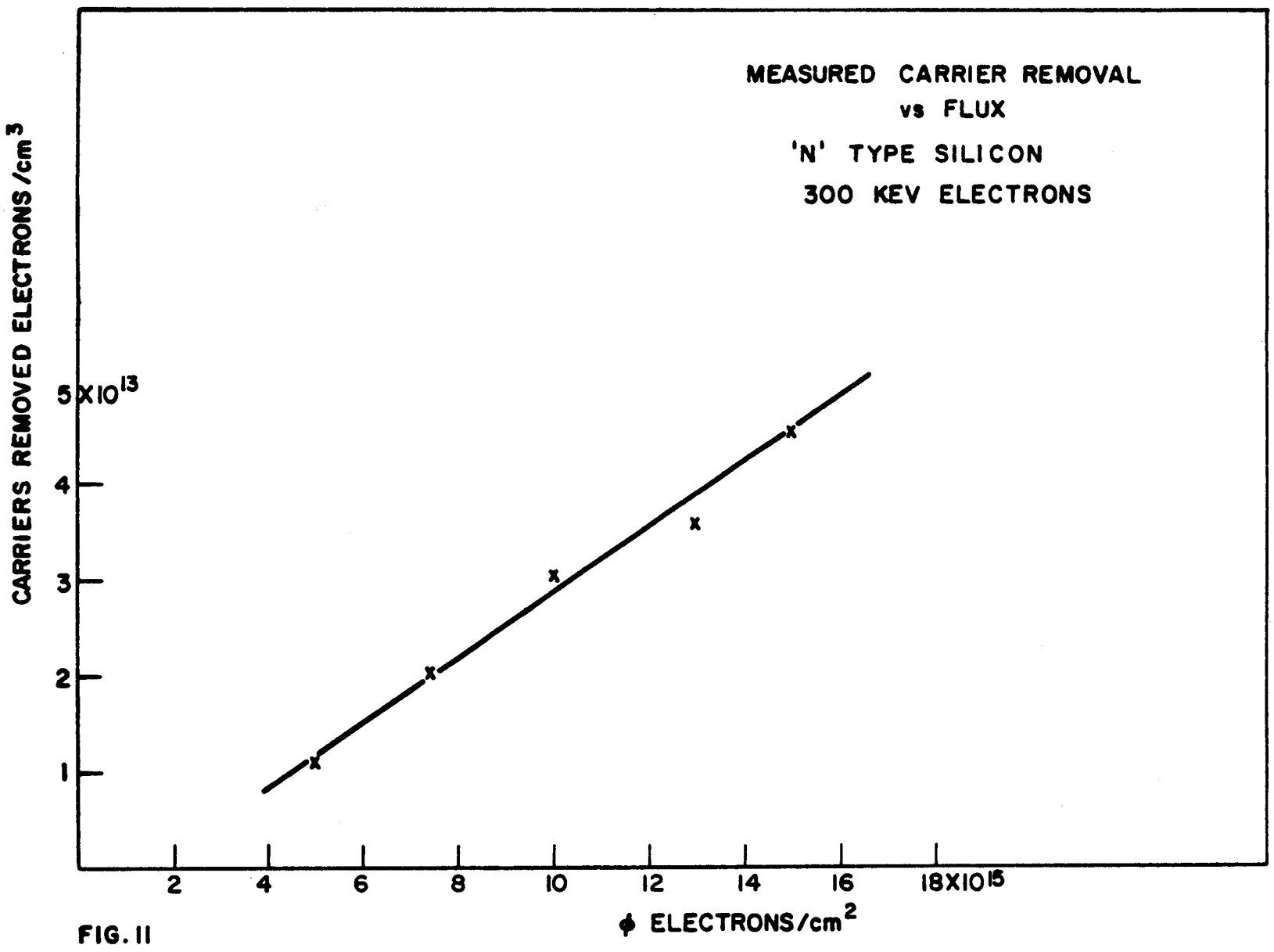
MEASURED CARRIER REMOVAL
vs FLUX
'N' TYPE SILICON
300 KEV ELECTRONS
CARRIERS REMOVED ELECTRONS/cm3
5X10^13
4
3
2
1
2
4
6
8
10
12
14
16
18X10^15
ϕ ELECTRONS/cm2

FIG. 11

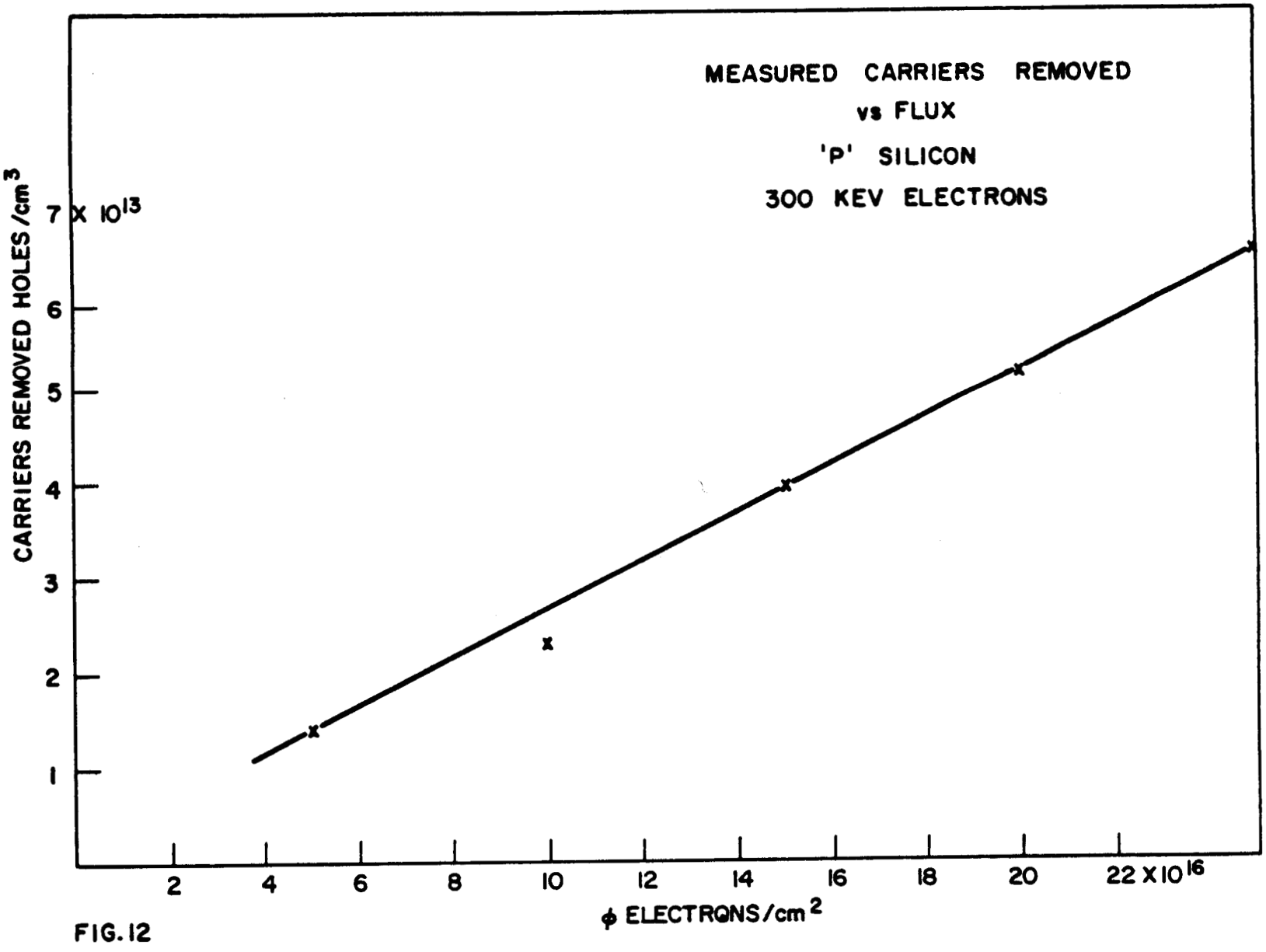
MEASURED CARRIERS REMOVED
vs FLUX
'P' SILICON
300 KEV ELECTRONS
CARRIERS REMOVED HOLES/cm3
7 X 10^13
6
5
4
3
2
1
2
4
6
8
10
12
14
16
18
20
22 X 10^16
φ ELECTRONS/cm2

FIG. 12

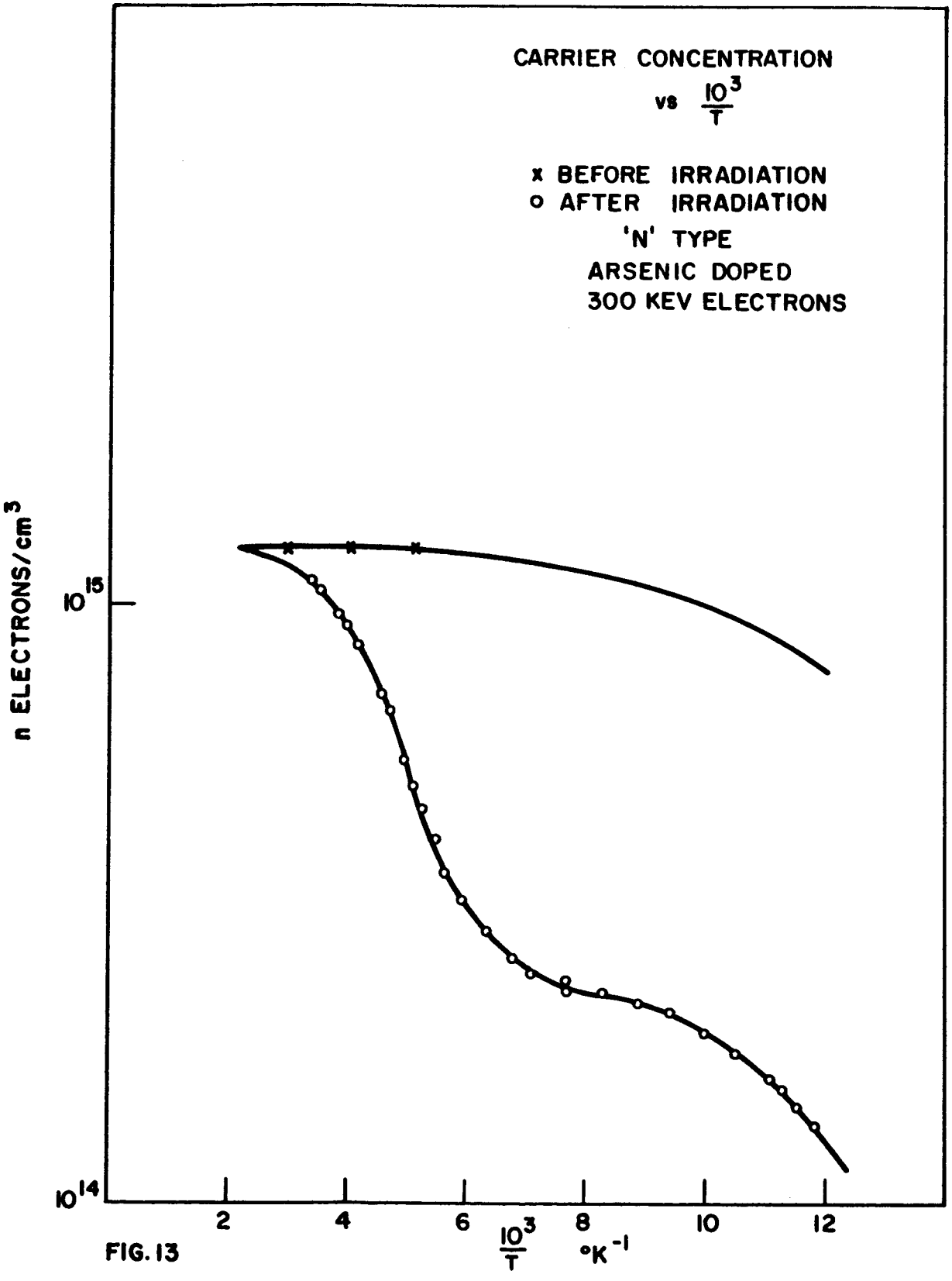
CARRIER CONCENTRATION
vs $\frac{10^3}{T}$
x BEFORE IRRADIATION
o AFTER IRRADIATION
'N' TYPE
ARSENIC DOPED
300 KEV ELECTRONS
n ELECTRONS/cm^3
10^{15}
10^{14}
2
4
6
8
10
12
$\frac{10^3}{T}$ °K^{-1}

FIG. 13

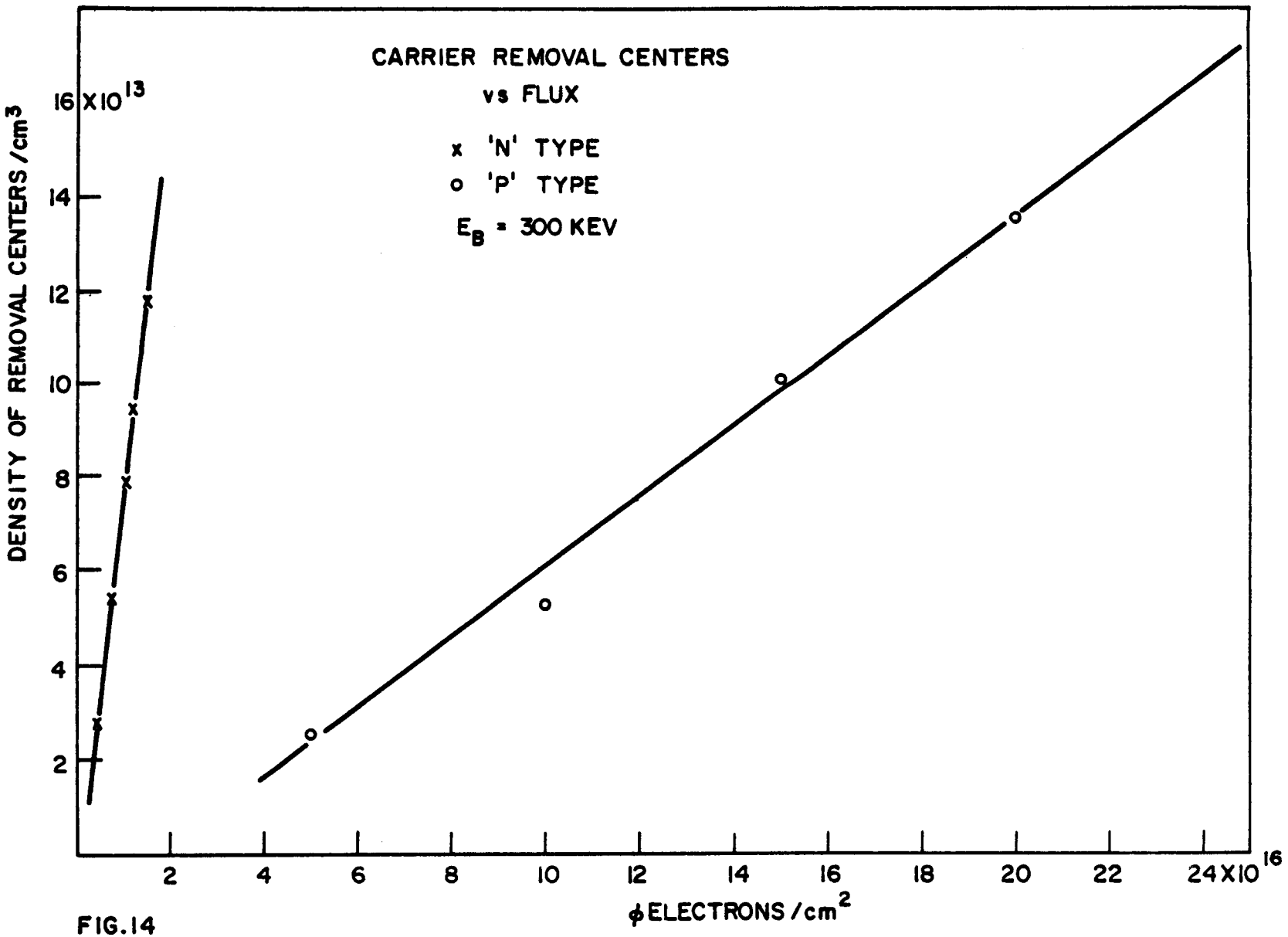
CARRIER REMOVAL CENTERS
vs FLUX
x 'N' TYPE
o 'P' TYPE
E_B = 300 KEV
DENSITY OF REMOVAL CENTERS /cm^3
16 X10^{13}
14
12
10
8
6
4
2
2
4
6
8
10
12
14
16
18
20
22
24X10^{16}
ϕELECTRONS /cm^2

FIG.14

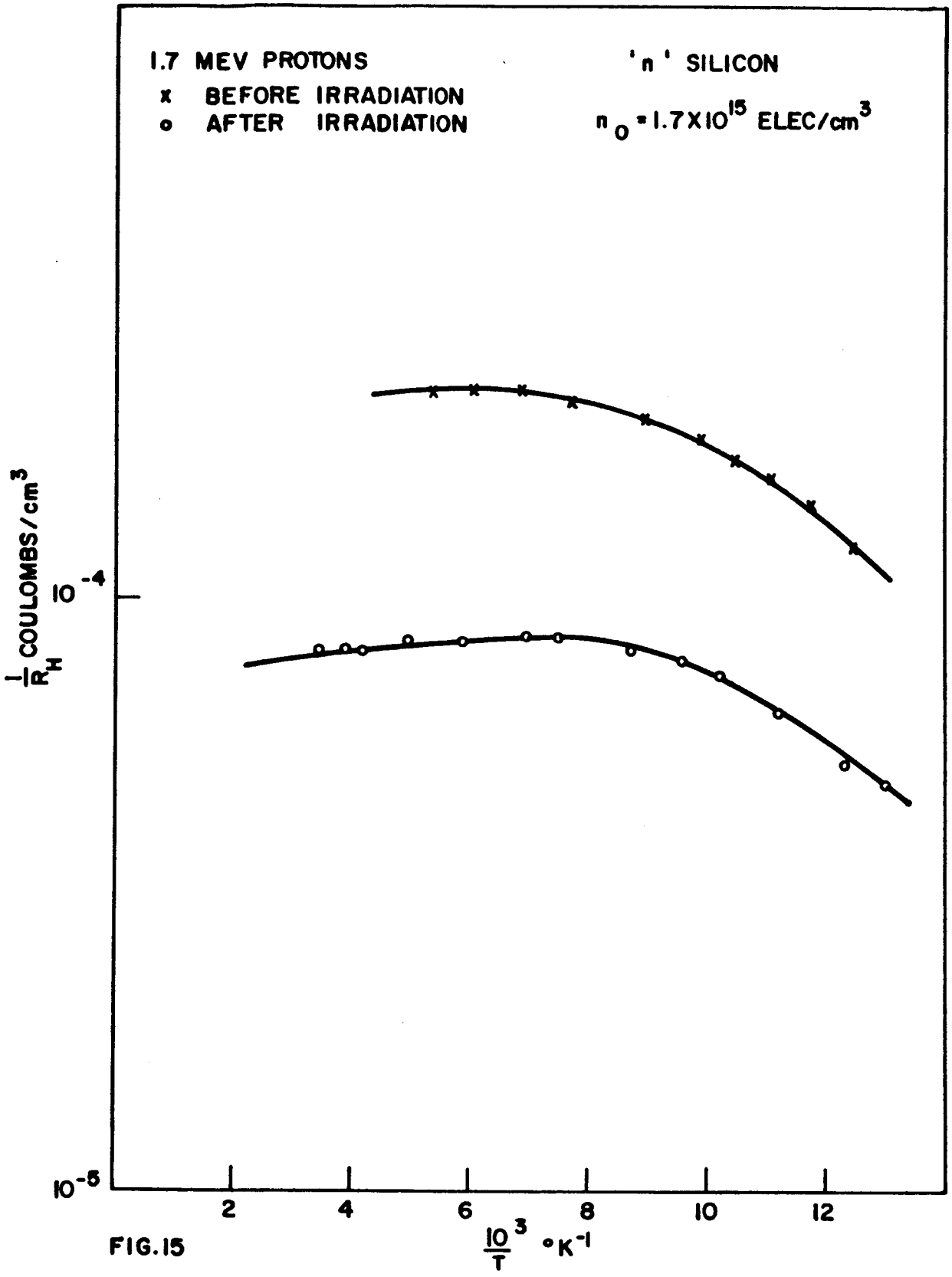
1.7 MEV PROTONS
'n' SILICON
x BEFORE IRRADIATION
o AFTER IRRADIATION
$n_0 = 1.7 \times 10^{15}$ ELEC/cm^3
$\frac{1}{R_H}$ COULOMBS/cm^3
10^{-4}
10^{-5}
2
4
6
8
10
12
$\frac{10^3}{T}$ °K^{-1}

FIG. 15

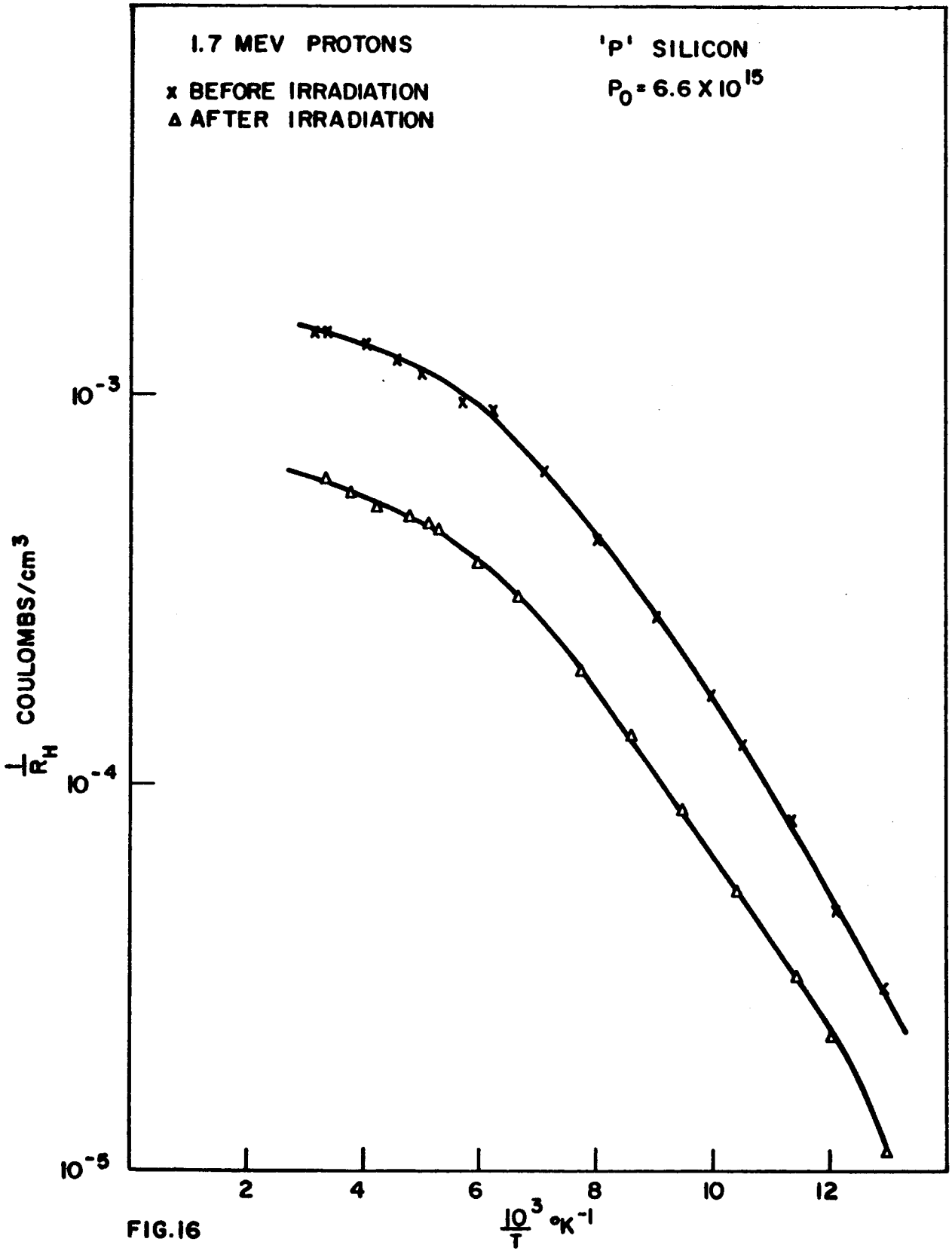
1.7 MEV PROTONS
'P' SILICON
x BEFORE IRRADIATION
Δ AFTER IRRADIATION
$P_0 = 6.6 \times 10^{15}$
10^{-3}
10^{-4}
10^{-5}
$\frac{1}{R_H}$ COULOMBS/cm^3
2
4
6
8
10
12
$\frac{10^3}{T}$ °K^{-1}

FIG.16

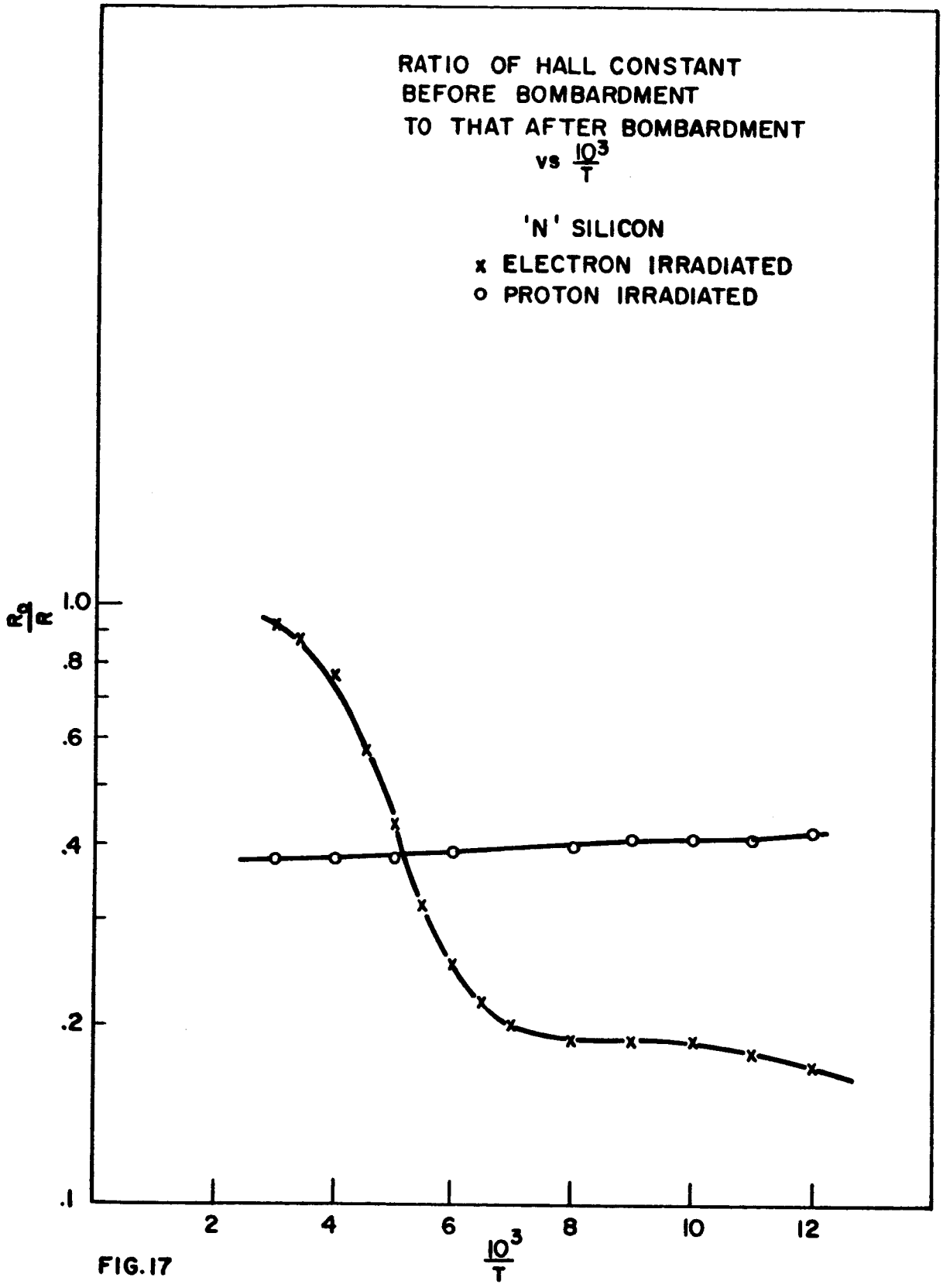
RATIO OF HALL CONSTANT
BEFORE BOMBARDMENT
TO THAT AFTER BOMBARDMENT
vs $\frac{10^3}{T}$
'N' SILICON
x ELECTRON IRRADIATED
o PROTON IRRADIATED
$\frac{R_0}{R}$
1.0
.8
.6
.4
.2
.1
2
4
6
8
10
12
$\frac{10^3}{T}$

FIG. 17

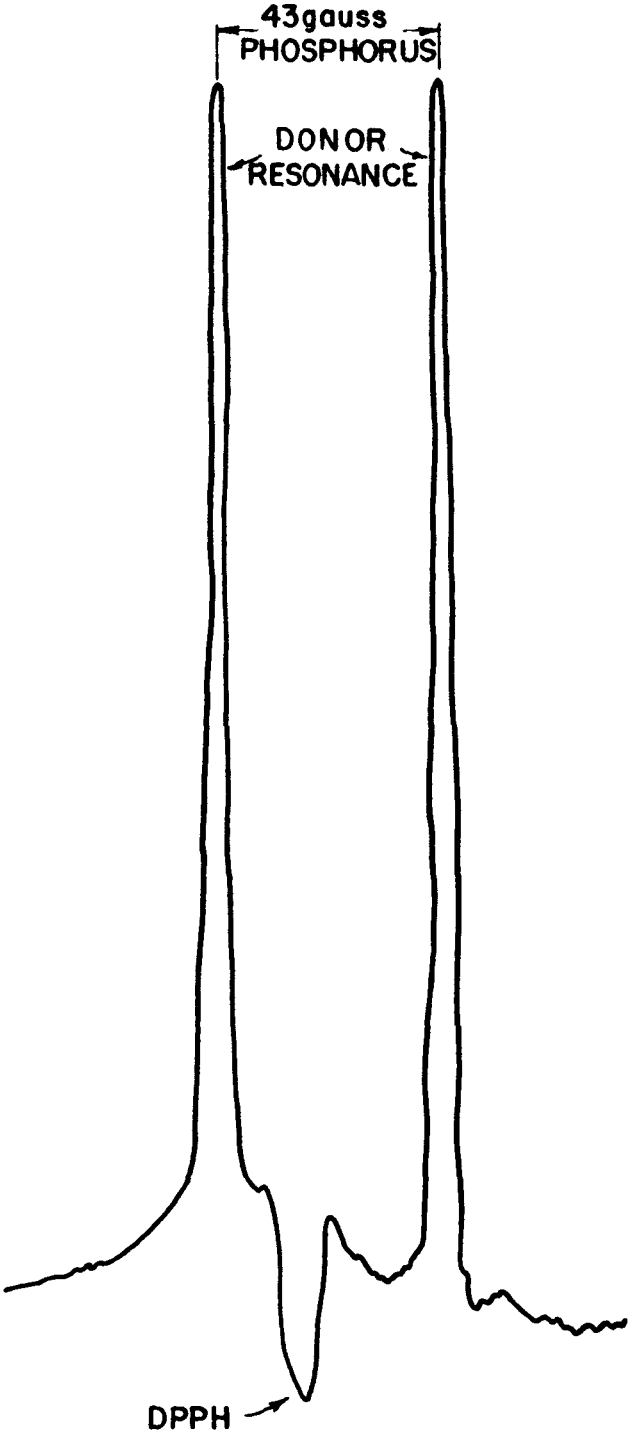

PHOSPHORUS DONOR RESONANCE IN 1Ω CM. UNIRRADIATED SILICON T = 4.2°K

FIG.18

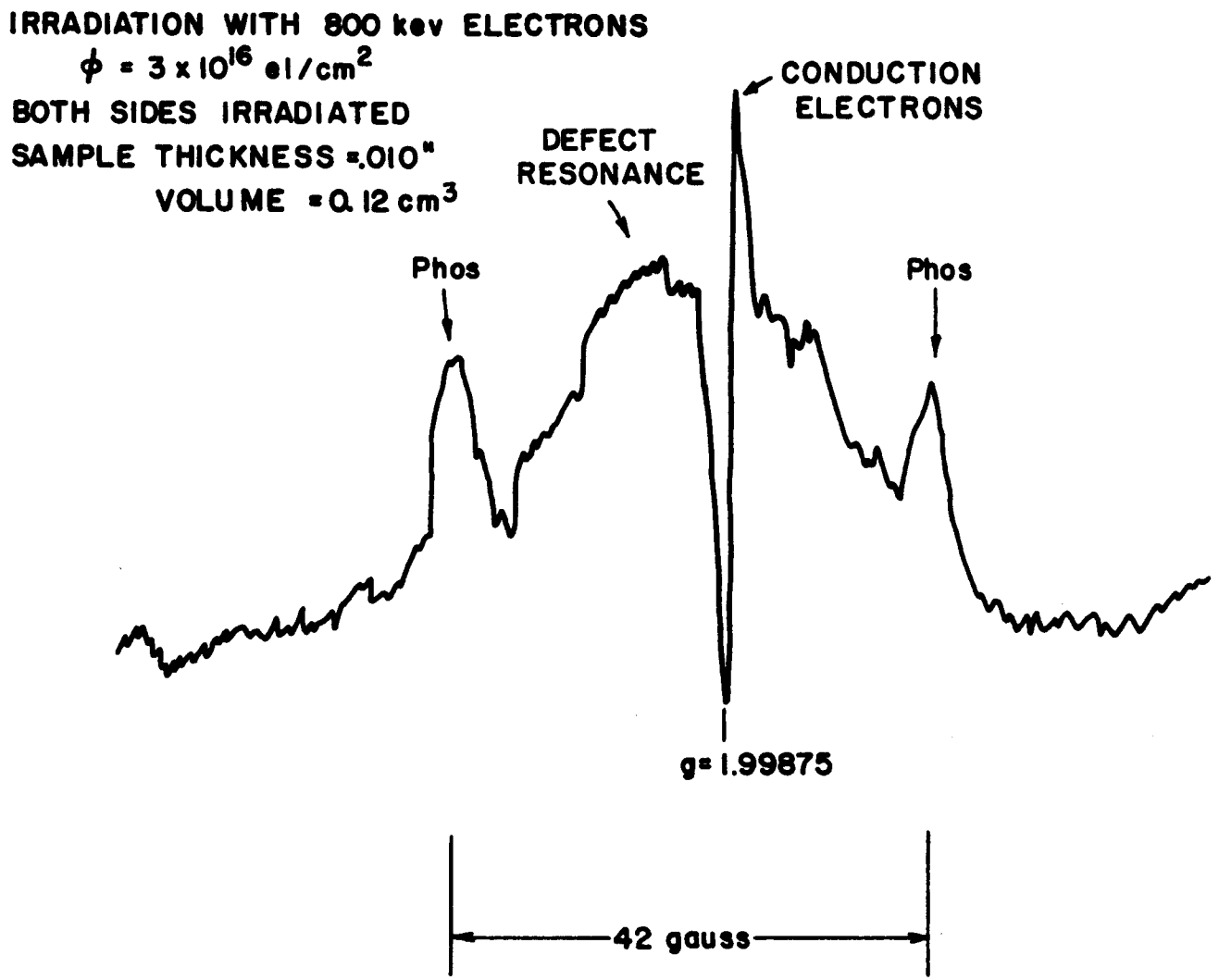

PHOSPHORUS DONOR RESONANCE AND DEFECT RESONANCE IN 1Ω CM. IRRADIATED SILICON T= 4.2°K

FIG. 19

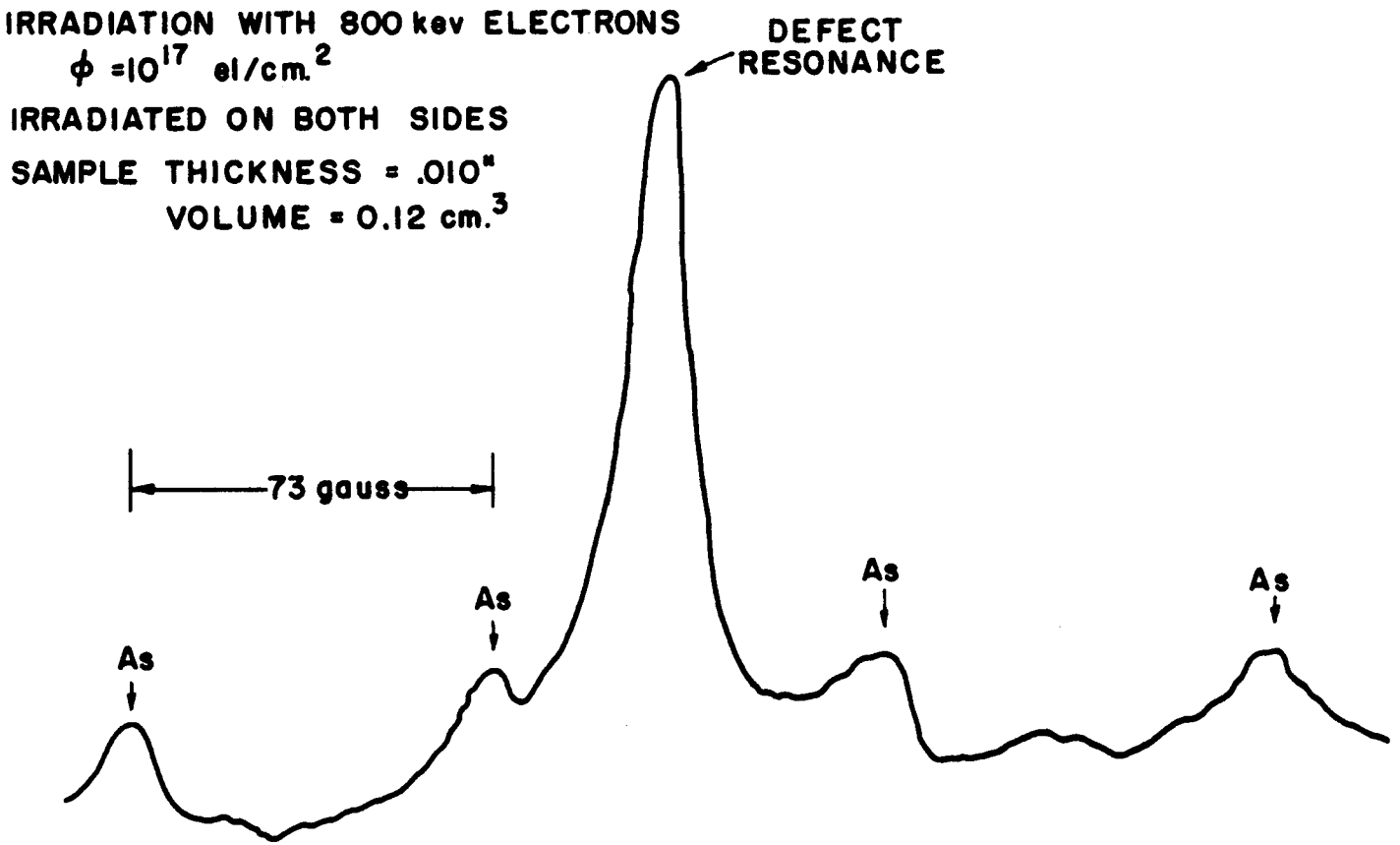

As DONOR RESONANCE AND DEFECT RESONANCE IN 1Ω CM IRRADIATION SILICON

FIG. 20